Mid-IR Microresonator-Based Optical Frequency Combs

Andrey Matsko
OEwaves Incorporated

09/01/2015
Final Report

REPORT DOCUMENTATION PAGE

1. REPORT DATE *(DD-MM-YYYY)*	2. REPORT TYPE	3. DATES COVERED *(From - To)*

4. TITLE AND SUBTITLE

5a. CONTRACT NUMBER

5b. GRANT NUMBER

5c. PROGRAM ELEMENT NUMBER

6. AUTHOR(S)

5d. PROJECT NUMBER

5e. TASK NUMBER

5f. WORK UNIT NUMBER

7. PERFORMING ORGANIZATION NAME(S) AND ADDRESS(ES)

8. PERFORMING ORGANIZATION REPORT NUMBER

9. SPONSORING/MONITORING AGENCY NAME(S) AND ADDRESS(ES)

10. SPONSOR/MONITOR'S ACRONYM(S)

11. SPONSOR/MONITOR'S REPORT NUMBER(S)

12. DISTRIBUTION/AVAILABILITY STATEMENT

13. SUPPLEMENTARY NOTES

14. ABSTRACT

15. SUBJECT TERMS

16. SECURITY CLASSIFICATION OF:			17. LIMITATION OF ABSTRACT	18. NUMBER OF PAGES	19a. NAME OF RESPONSIBLE PERSON
a. REPORT	b. ABSTRACT	c. THIS PAGE			
					19b. TELEPHONE NUMBER *(Include area code)*

Standard Form 298 (Rev. 8/98)
Prescribed by ANSI Std. Z39.18

AFOSR

Mid-IR Microresonator-Based Optical Frequency Combs

Final Report
06/01/12 – 05/31/15

Dr. Andrey Matsko,
Principal Investigator

OEwaves Inc.,
465 N Halstead Street, Ste 140,
Pasadena, CA 91107
and
The Aerospace Corp.,
2310 El Segundo Blvd,
El Segundo, CA 90245

Contract Number:
FA9550-12-C-0068

Table of Contents

1. Introduction

This document contains Final Report pertaining to work performed in "Mid-IR Microresonator-Based Optical Frequency Combs" program, funded by AFOSR (Contract No. FA9550-12-C-0068) and executed by OEwaves, Inc. ("OEwaves") and The Aerospace Corporation ("Aerospace").

The effort was aimed at investigating fundamental properties of frequency combs (Kerr combs) generated by cascading parametric nonlinear effects in whispering gallery mode (WGM) crystalline microresonators.

The main goals for the work were (a) theoretical extraction of microresonator design parameters and specifications enabling the generation of Kerr combs in the mid-infrared (mid-IR) wavelength region and (b) demonstration of a mid-IR Kerr comb obtained by pumping a whispering gallery mode microresonator with a 4.5µm quantum cascade laser (QCL), which amounts to the longest-wavelength Kerr comb to date and first to access the molecular fingerprint region of the optical spectrum, a critical enabler for a wide range of new military and civilian chemo/bio sensing applications.

2. Major Accomplishments

In this effort we performed a broad theoretical and experimental study of properties of microcavity Kerr frequency combs that led to publication of 14 refereed papers in Nature Communications, Optica, Optics Letters, etc. One more paper is currently under consideration in Laser & Photonics Review. In particular, the Project resulted in the following breakthroughs in the field of linear and nonlinear mid-IR optics:

➢ We observed generation of frequency combs centered at 4.5µm in high-finesse CaF_2 and MgF_2 whispering gallery mode resonators pumped with quantum cascade lasers. A frequency comb broader than a half of an octave was demonstrated when ~20mW of pump power was coupled to an MgF_2 resonator characterized with quality factor $> 10^8$. This is the longest-wavelength Kerr comb achieved to date.

➢ We demonstrated quantum cascade lasers stabilized to high-Q crystalline mid-IR microcavities. The lasers operating at room temperature at around 4.5 µm have linewidth approaching 10 kHz along with excellent spectral purity and are promising for on-chip mid-IR and IR spectrometers.

3. Objectives

No changes to the objectives of the research effort were introduced. The objectives are listed below.

(1) Develop analytical and numerical models that elucidate how group velocity dispersion (GVD) affects key aspects of Kerr comb generation, including threshold power, repetition rate, overall comb spectral bandwidth, and temporal coherence. Derive solutions of the nonlinear differential equations describing the frequency comb generation, and analyze the solution stability in the case of anomalous, zero or normal net GVD. Determine the relationship between GVD and selected resonator mode families.

(2) Improve existing analytical models of Kerr combs by formulating a theoretical treatment of Kerr comb amplitude and phase fluctuation dynamics. Determine which set of requirements must be met in order to obtain mode-locked (coherent) octave spanning Kerr combs and explain why recently generated octave-spanning combs are incoherent.

(3) Find the best resonator parameters for generation of wide and stable combs with high comb-line visibility. Tailor the theoretical analysis to finding microresonator parameters required for both spectrally wide and stable mid-IR frequency combs. Investigate materials suitable for comb generation at such wavelengths and quantitatively study the effect of the resonator morphology and mode characteristics on its GVD, with the goal of creating ideal conditions for mid-IR comb generation in well-established materials such as MgF_2 and CaF_2.

(4) Formulate an optimized design of microresonator morphology and corresponding coupling optics to achieve efficient coupling of mid-IR pump light into the microresonator and low-threshold mid-IR Kerr comb generation. Fabricate and package the ultra-high-Q microresonator according such design and make it transportable from OEwaves to Aerospace without degradation to the Q factor.

(5) Investigate and demonstrate experimentally the coupling/locking of a mid-IR-wavelength, extended-cavity quantum cascade laser (EC-QCL) to a high-Q microresonator optical mode. In particular, study the effectiveness of passive (self-injection and thermal) and active (Pound-Drever-Hall) locking schemes. Measure the linewidth, stability, and amplitude noise of the microresonator-locked QCL. Investigate, theoretically and experimentally, the properties of fabricated micro-resonators in the mid-IR. Measure their Q-factors and explain the observations.

(6) Demonstrate experimentally a Kerr frequency comb in the mid-IR centered at ~4.5μm, using an EC-QCL as the pump source. Circumvent the unavailability of mid-IR optical spectral analyzers and/or multi-GHz-bandwidth by implementing interferometric techniques in the spectral/temporal characterization of the mid-IR comb. Use this detection apparatus to measure the mid-IR Kerr comb coherence and study phase locking of the comb harmonics. Characterize the amplitude and phase noise of the comb and compare it to the theory.

(7) Investigate theoretically the generation of coherent Kerr combs spanning an octave or more in the mid-IR. Use the results of this analysis to derive a detailed design for an experimental demonstration of a mid-IR octave-spanning coherent Kerr comb.
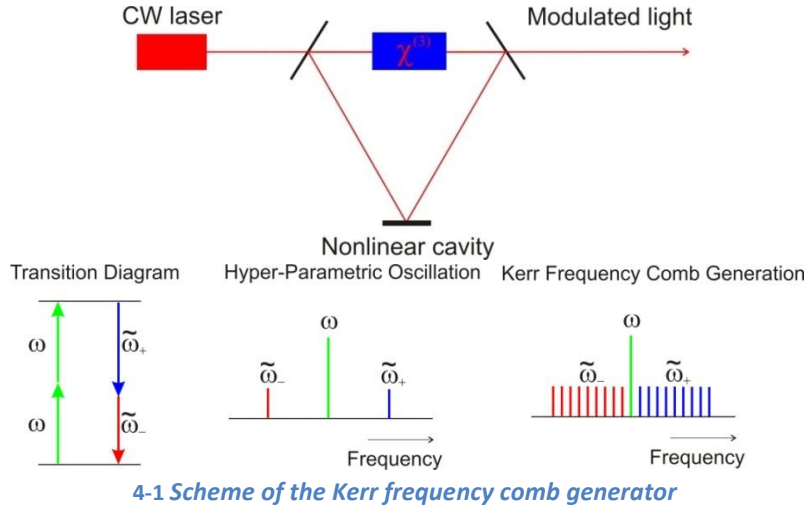
4. Accomplishments

This section summarizes our achievements made towards the project Objectives.

Fundamentals of Kerr Combs and WGM Resonators

Model
The baseline laser/microresonator configuration we considered in our Kerr comb generation model is schematically illustrated in Fig. 4-1.

4-1 *Scheme of the Kerr frequency comb generator*

Kerr comb generation in solid-state optical microresonators stems from a four-wave mixing (FWM) process reminiscent of modulation instability and parametric oscillation in optical fibers. FWM is a nonlinear optical effect consisting of creation of frequency-domain sidebands, which surround the frequency of the laser coupled to the microresonator. The sidebands are separated approximately by integer numbers of free spectral ranges (FSRs) of the resonator and normally equidistant from and symmetrically placed around the central laser frequency.

In order to numerically model Kerr frequency comb formation, we utilize a set of equations for light localized in discrete modes of the microresonator. The starting point is the standard Hamiltonian, $\hat{V}$, describing the interaction between light and microresonator:

$$\hat{V} = -\frac{hg}{4\pi}(\hat{e}^+)^2\hat{e}^2 \quad , \quad \hat{e} = \sum_N \hat{a}_j$$

(1)

Here, g is the light-matter coupling parameter and $\hat{e}$ denotes the overall photon annihilation operator, expressed as the sum of annihilation operators corresponding to individual microresonator modes, each labeled as $\hat{a}_j$. For the purpose of numerical simulations, we chose to use N = number of modes = 101 (i.e. the pumped mode matched to the laser frequency plus 100 adjacent modes).

Based on the form of the Hamiltonian *V*, we can derive "equations of motion", i.e. equations for the time-dependent evolution of the optical field, in the following form

$$\frac{d}{dt}\hat{a}_j = -(\gamma + i\omega_j)\hat{a}_j + \frac{2\pi i}{h}[\hat{V}, \hat{a}_j] + Fe^{-i\omega t}\delta_{(N+1)/2.j}$$

(2)

Here, γ is the half width at half maximum common to all microresonator modes, ω$_j$ is the central frequency of the jth mode, *h* is Planck's constant, *F* is the normalized pump laser amplitude, and δ is the Kronecker delta operator.
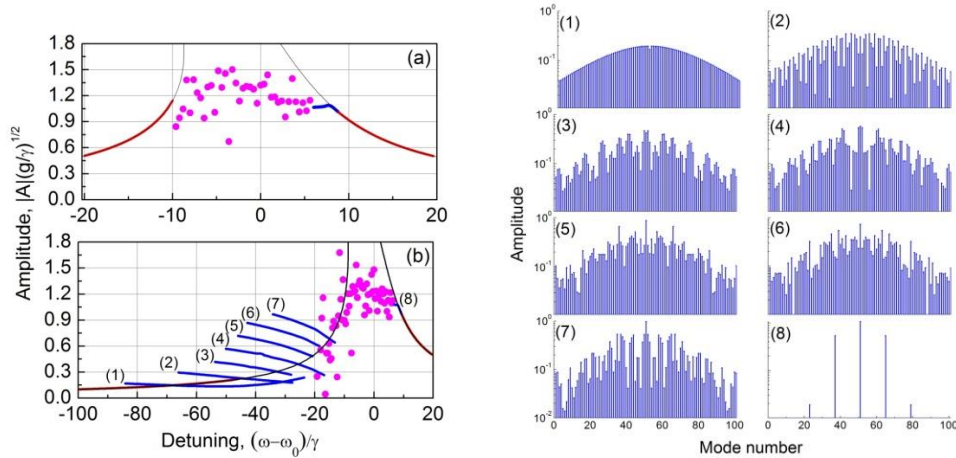
4-2 Left: Normalized field amplitude in the optically pumped mode vs. frequency of the CW pump light. Solid lines show stable branches corresponding to generation of various Kerr combs, dots correspond to generation of chaotic combs or combs with time-depending envelopes. Plot (a) refers to a soft excitation regime (<1 photon per mode). Plot (b) refe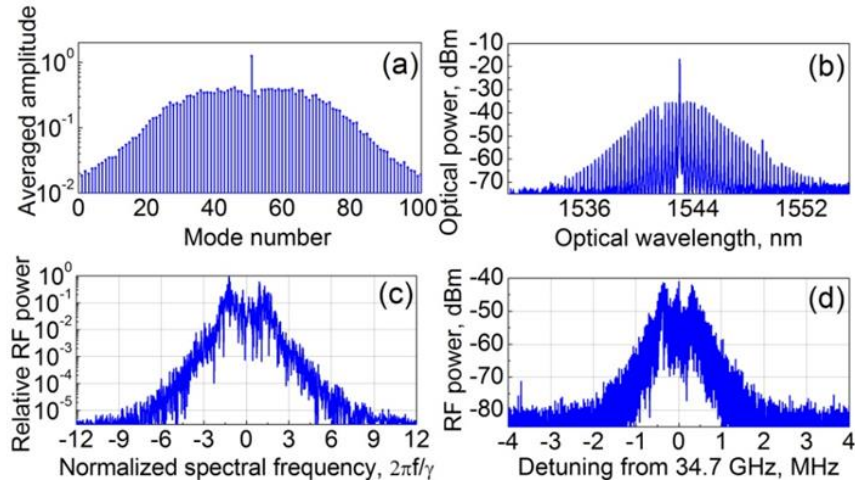rs to hard excitation. Stable solutions are realized for the particular nonzero initial condition and detuning selection. The comb can also be excited from nearly zero initial excitation of modes, if the pump frequency is shifted non-adiabatically, as shown in Fig. 4. Constant tuning of the pump frequency also permits to observe solutions corresponding to the stable branches. Right: Simulated spectra of the combs corresponding to stable-solution branches shown in the left panel, plot (b). For further details, see A. Matsko et al. Optics Letters 38, 525 (2013).

Chaotic combs

Numerical solutions of Eq. (2) showed that a chaotic comb generation regime characterized by a temporally unstable, spectrally asymmetric, and incoherent comb envelope is generally accessible for a wide range of initial conditions, as documented in Fig. *4-2*. Interestingly, such chaotic solutions can be mistaken for stable, symmetric, coherent combs when experimentally observed with a standard optical spectrum analyzer (OSA). This artifact stems from millisecond-scale time averaging performed by OSAs, which masks the faster dynamics of the chaotic comb. Conversely, the corresponding comb-produced beat note, observed with a radio-frequency (RF) spectrum analyzer, is noisy, irregular, and significantly wider than the linear bandwidth of microresonator modes.

We confirmed the existence of a chaotic Kerr combs through numerical simulation and matching experiment, as shown in Fig. 4-3. We also found that "regular", coherent Kerr combs cannot be generated when no pump photons are initially present in the FWM sidebands i.e. when the sidebands originate from mere quantum fluctuations (parametric noise).

Contract No:
FA9550-12-C-0068   OEwaves, Inc.   6

Distribution Statement A. Approved for public release, distribution is unlimited.

4-3 *Optical spectrum of an incoherent Kerr comb [(a),(b)] and associated RF signals [(c),(d)] generated by the comb on a fast photodiode. (a) and (c) represent simulation results, whereas (b) and (d) are measurement results. To simulate the spectrum of the chaotic comb (a), we time averaged the chaotic comb spectra over time = 100/γ. This averaging corresponds to the averaging introduced by an OSA used to observe the comb spectrum in the experiment.*

To produce a coherent comb using a single-frequency pump laser, one needs to change in a non-adiabatic fashion either the power or the detuning of the pump light. Figure 4-4 exemplifies the simulated emergence of a regular, coherent comb from initially chaotic oscillations when the pump laser frequency suddenly moves to a position where regular solutions are allowed. The modification of the oscillation regime is accompanied by intricate transient comb dynamics which are identified for the first time in our analysis.
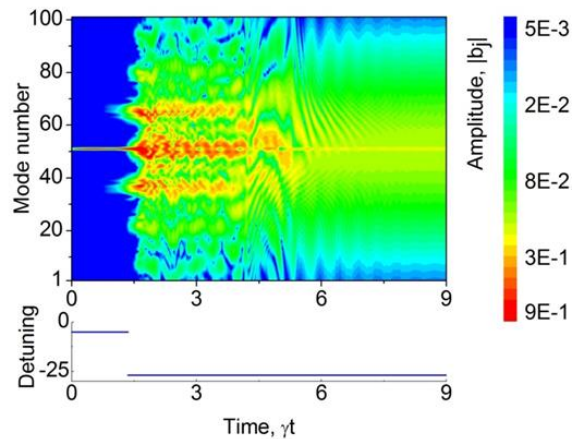
4-4 *Density plot showing the time dependence of amplitude of comb harmonics. This is an example of excitation of a regular frequency comb in an empty microresonator via non-adiabatic change of the oscillator parameters. When the detuning is modified (from -5 to -27 HWHM of the selected WGM, in this case), the abrupt change results in the generation of a regular, broad coherent comb.*
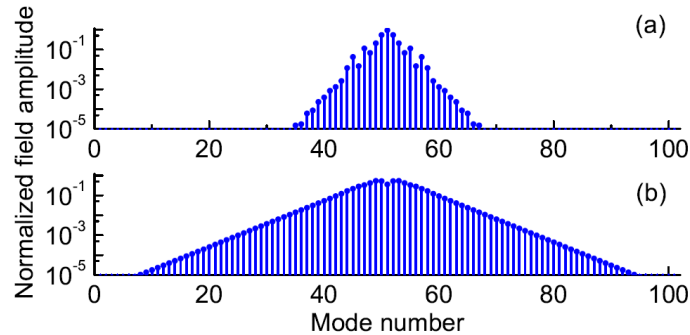
4-5 Spectrum of amplitudes of optical harmonics of the frequency comb generated in a microresonator. The narrowest and widest spectra are presented in plots (a) and (b).

Breather solitons

Our numerical analysis also showed that Eq. (2) admits breather soliton solutions, including Kuznetsov-Ma solitons, which are known solutions of the nonlinear Schrodinger equations and can form in high-finesse microresonators for specific values of the pump beam frequency and power. In fact, we argue that the relatively slow time-domain modulation of Kerr comb frequency harmonics, observed in several recent experiments, can be attributed to such soliton formation.

The temporal envelope of the pulse and corresponding spectral width of the frequency comb forming the pulse slowly varies in time as well as propagation distance in the case of KM solitons (see Figures *4-5* and *4-6*). Such a behavior is known to be an example of Fermi-Pasta-Ulam recurrence. Since demodulation of the pulses on a fast photodiode would result in generation of low frequency RF harmonic, along with high frequency harmonics corresponding to the pulse repetition rate, we argue it is possible that resonant breathers were already generated in microresonators, and proper experimental techniques are needed for their observation.
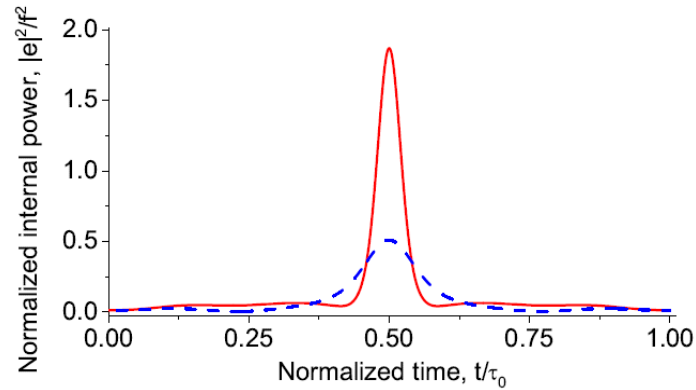
4-6 The shortest (red solid line) and longest (blue dashed line) optical pulses generated in the resonator for the spectra shown in Fig. 6.

Kerr frequency comb generation in overmoded resonators

Another result of our numerical analysis has been the elucidation of the process of Kerr comb formation in certain experimentally observed conditions, which include relatively small (<100 GHz) comb spacing, "soft" excitation (i.e. negligible pump power is initially present in all modes except the one being directly pumped), and zero or normal GVD. We found that such combs originate from the   interaction (mainly driven by unavoidable imperfections in the microresonator structure) among resonator modes belonging to different mode families overlapping within the same spatial volume.

Such interactions are to be expected in all "overmoded" microresonators, which support more than one mode family and indeed represent the majority of microresonators experimentally characterized in the literature to date.

Our analysis, detailed in A.A. Savchenkov *et al.*, Optics Express **20**, 27290 (2012), shows that scattering-based interaction among nearly degenerate optical modes is the key factor explaining the low-threshold generation of Kerr combs in resonators exhibiting small and/or large normal GVD. The mode interaction is found capable of effecting drastic changes in the local GVD, resulting in either a significant reduction or increase of the oscillation threshold.

We performed an experiment with a large, overmoded microresonator of near-zero GVD and observed generation of the frequency combs with envelopes similar to the ones predicted by the theory (see Fig. *4-7* and Fig. 4-8).
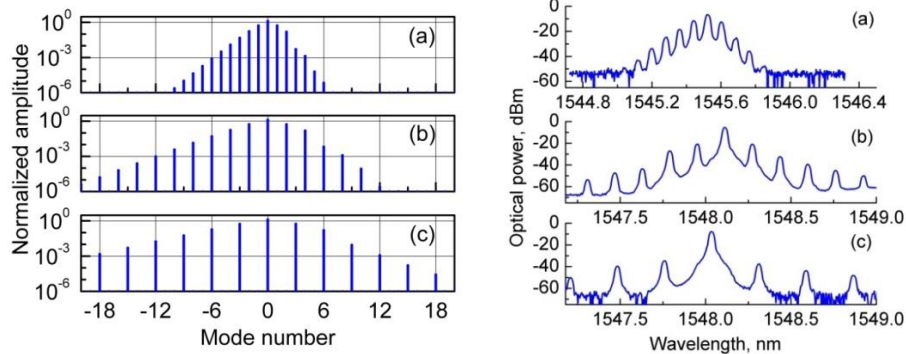
4-7 Left: Examples of numerically simulated Kerr combs in overmoded microresonators characterized by near-zero GVD and having the frequency of one mode shifted by inter-modal interactions. Right: Experimental spectra of three Kerr combs observed in the same overmoded WGM resonator when light is coupled to three arbitrary modes having strong interaction with other modes within the resonator. The wavelength of the pump light was changed to select specific modes, and depending on the mode selected, we observed: (a) single-FSR, (b) dual-FSR comb, and (c) triple-FSR combs. (see A. Savchenkov et al., Opt. Express 20, 27290-27298 (2012) for details)
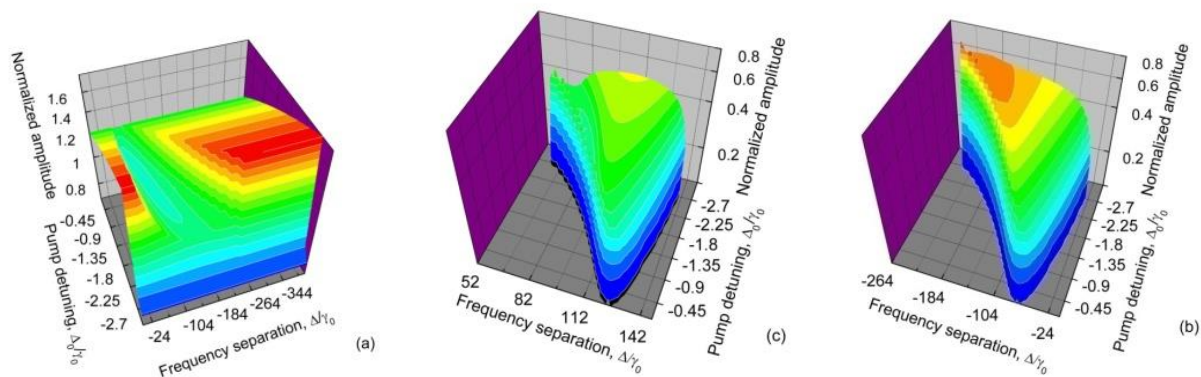
4-8 Amplitude distribution for the pump mode (a) and first two sidebands [(b) and (c)] of Kerr combs based on mode interaction. The sidebands are apparently unequal at any pump frequency detuning from the pumped optical mode as well as frequency separation (see Fig.8) between the two interacting modes resulting in local modification of the GVD of the microresonator.

In our experiment we used a calcium fluoride (CaF$_2$) resonator having diameter = 6.721mm. The resonator had approximately 9.9 GHz free spectral range (FSR) and had loaded quality factor exceeding 10^9. We pumped the resonator with 1545.5nm-wavelength light emitted by a distributed feedback semiconductor laser. The light was coupled to the resonator via a coupling prism. The optical power emitted by the laser was 15 mW, and 3.2-1 mW of the light entered the selected modes of the resonator (the values depend on the mode selection). The output light was collected using a PM Panda fiber and forwarded to an optical spectrum analyzer.

The measured spectra are shown in Fig. *4-7* and 4-9. It is worth recalling here that, in a resonator with near-zero normal GVD, frequency comb generation would be impossible unless mode interaction is assumed or optical seed is used to facilitate the hard excitation of the oscillation process.
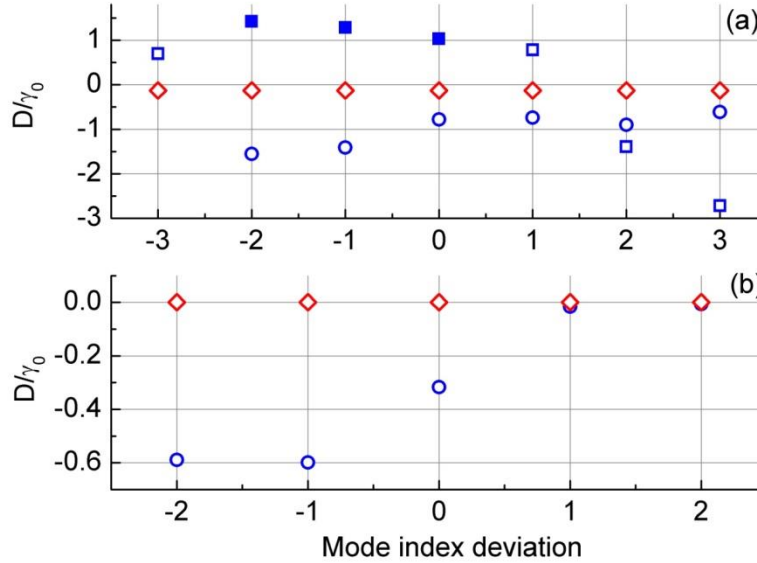
4-9 Measured GVD and Kerr frequency comb generation correlation. The measurement accuracy of the resonator spectrum is on the order of 10 Hz. (a) GVD parameter D (see A. Savchenkov et al., **Opt. Express 20, 27290-27298 (2012) for details***) for a CaF$_2$ WGM resonator with 30 GHz free spectral range and 25 kHz loaded bandwidth. Two mode families are studied (data are shown by circles and squares). The comb generation is observed only in the modes corresponding to filled squares, when parameter D exceeds 1. (b) GVD parameter D for a CaF$_2$ WGM resonator with 10 GHz free spectral range and 78 kHz loaded bandwidth. No comb generation is detected and D is always smaller than 0. Red diamonds stand for the theoretical value of the GVD parameter with no mode crossing taken into account.*

Transient regime of Kerr comb formation

The temporal growth of an optical Kerr frequency comb generated in a microresonator was studied both experimentally and numerically. We found that combs emerge from vacuum fluctuations of the electromagnetic field on time scales significantly exceeding the ring-down time of the resonator modes. The frequency harmonics of the comb spread starting from the optically pumped mode if the microresonator exhibits anomalous GVD. The harmonics have different growth rates resulting from a sequential four-wave mixing process that explains intrinsic mode locking of the comb (Fig. *4-10*).
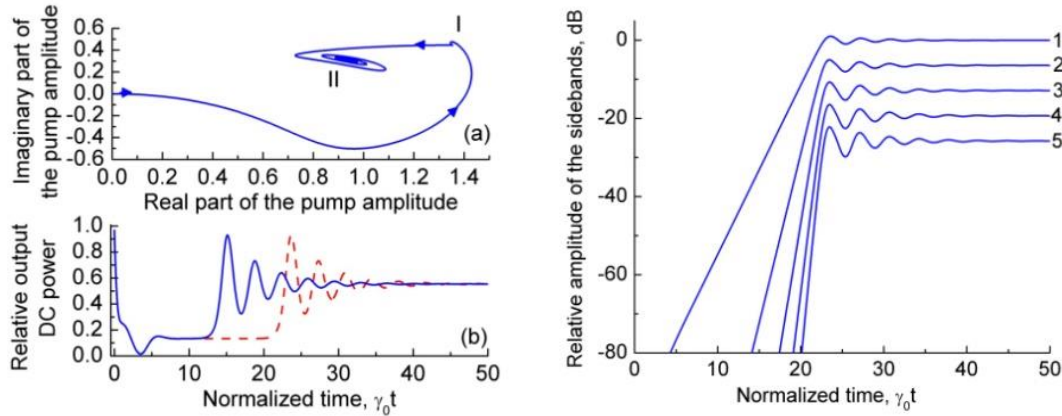
4-10 (a) Transient behavior of the normalized amplitude of the electromagnetic field of the externally pumped optical mode. (b) The transient behavior of the light exiting the resonator is calculated for slightly over coupled modes, and for different values of nonlinearity/power. The oscillator reaches its steady state faster for larger nonlinearity/power, and slower for smaller nonlinearity/power.

The transient behavior of the Kerr frequency comb can be verified experimentally if one measures the power of the comb harmonics exiting the resonator. Instead of the direct measurement of the optical harmonics, the power of the radio frequency (RF) signal generated on a fast photodiode by the comb can be measured. We performed such experiments, as detailed in A. A. Savchenkov *et al.*, Physical Review A **86,** 013838 (2012).
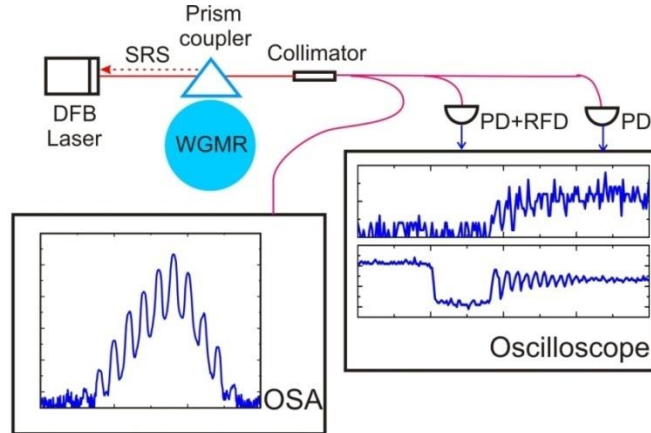
4-11 Schematic of the experimental setup. The WGM resonator is pumped with a DFB laser, self-injection locked to the selected mode. The output light is analyzed with an optical spectrum analyzer (OSA) showing the spectrum of the generated Kerr comb. Part of the light is sent to a fast photodiode (PD). The photocurrent, modulated with a frequency equal to the comb repetition rate, is directed to an RF power detector (RFD), and a fast oscilloscope. This signal is proportional to the convolution of the harmonics of the optical frequency comb. Some of the light is also detected with a slow photodiode (PD) and the photocurrent from this photodiode is forwarded to another channel of the same oscilloscope. This signal shows the integral DC power leaving the resonator. Comparing the signals with the fast oscilloscope we are able to measure the time delay between the generation of the Kerr comb and the moment the pump light enters the corresponding mode.

We used a calcium fluoride (CaF_2) whispering gallery mode (WGM) microresonator with loaded Q-factor of 2.2×10^9 (full width at the half maximum of the mode is 90 kHz, and corresponding ring down time 1.75µs). The intrinsic Q-factor of the resonator was 5.5×10^9, which means that the attenuation of light in the modes was primarily given by the interaction with the evanescent field coupler (a glass prism), and not by the scattering and loss of the resonator host material. The resonator was pumped using a 1545nm distributed feedback (DFB) semiconductor laser, self-injection locked to a selected resonator mode. The laser was emitting approximately 6mW of power, 30% of which entered the resonator (see Fig. *4-11* for a schematic view of the experimental setup). The observed variation of the Kerr frequency comb dynamics is illustrated by Figure *4-12*.
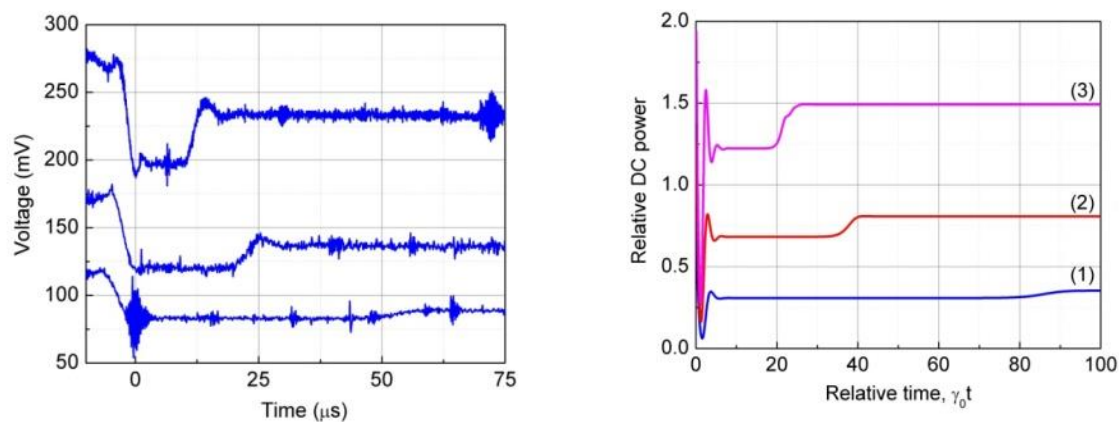
*4-12 Variation of the frequency comb dynamic when the same optical mode is pumped with different laser power. Left: Experimentally observed transient behavior of the Kerr frequency comb was measured via monitoring the power of the DC signal generated by the light exiting the resonator on a slow photodiode. The voltage at the photodiode is proportional to the power. Right: Same dependencies obtained via numerical simulation.*

The first demonstration of a Kerr frequency comb in a sapphire WGM resonator

Sapphire is another material transparent in mid-IR. We studied theoretically, and demonstrated experimentally, generation of coherent optical frequency combs in a sapphire WGM resonator (Fig. *4-13*). We verified phase locking of the comb harmonics by demodulating the comb on a fast photodiode and by observing production of a spectrally pure radio frequency signal. The sapphire resonator is an excellent candidate for on-chip device integration of the comb oscillator, because of excellent optical and superior mechanical properties of the material.
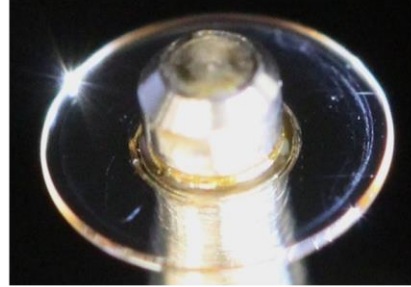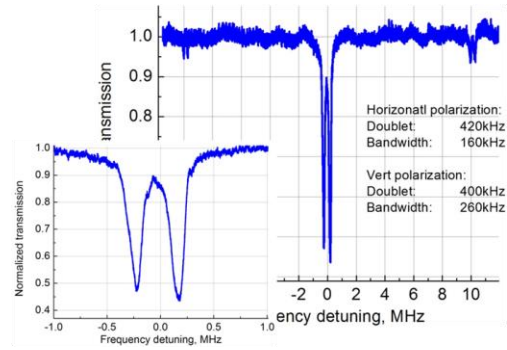
Proc. SPIE vol. 8960, pp. 896013-896013-10 (2014).

4-13 Demonstration of a sapphire WGM resonator: setup and optical spectra

We performed numerical simulations and shown that Kerr comb generation is possible in the resonator as the resonator has proper value and sigh of GVD (Fig. *4-14*).
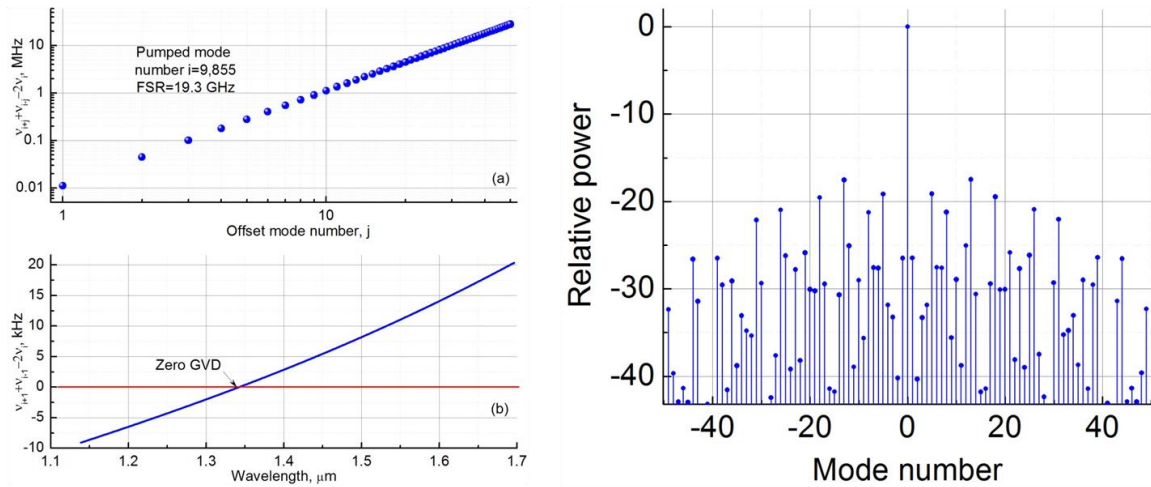
4-14 Results of theoretical analysis of the dispersive properties of the sapphire resonator (Left) and numerical simulations of a Kerr frequency comb that can be generated in the resonator (Right).

Contract No:
FA9550-12-C-0068   OEwaves, Inc.   14

Distribution Statement A. Approved for public release, distribution is unlimited.
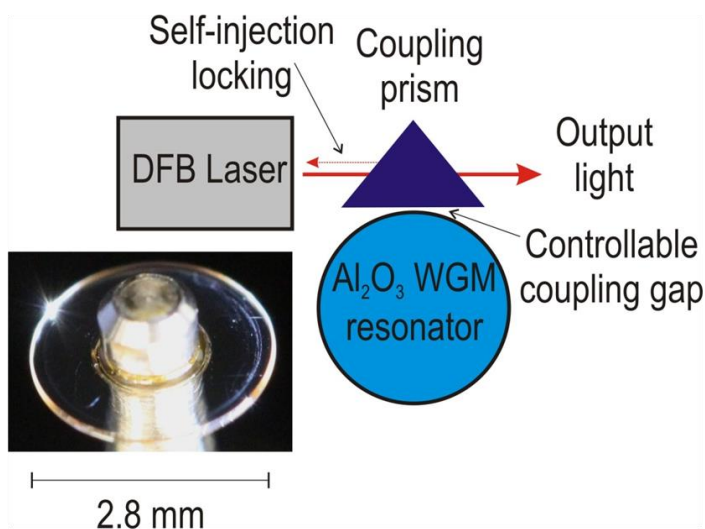
Proc. SPIE vol. 8960, pp. 896013-896013-10 (2014).

4-15 Left: Experimental setup used to generate and observe Kerr frequency comb in a sapphire WGM resonator. Right: Optical spectrum of the observed Kerr frequency comb as well as spectrum of the RF signal generated by the Kerr comb on a fast photodiode.

We observed generation of Kerr frequency comb by pumping the resonator with continuous wave light (Fig. *4-15*). The comb was demonstrated to be phase locked by demodulating it on a fast photodiode and generating a narrow RF beat note. To our knowledge, this is the first demonstration of generation of Kerr frequency comb in sapphire.

The sapphire frequency comb generators are particularly interesting because of the excellent mechanical and optical properties of the material. Monolithic sapphire resonators are much less prone to various environmental factors, when compared with other optical materials. For instance, because of substantially higher mechanical strength, these resonators are expected to produce oscillators with excepti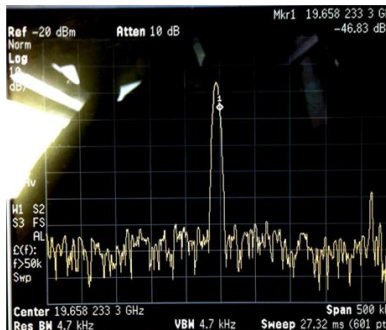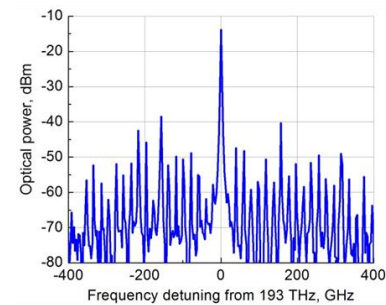onally low acceleration sensitivity, opening the way for applications on expanding range of mobile platforms. Furthermore, the relatively high refractive index of sapphire simplifies on-chip integration of the resonators. All these features point to the possibility of fabricating robust, chip-scale optical frequency comb generators based on sapphire. These resonators are also of interest as optical reference supercavities characterized with high quality factor in a broad wavelength range, and as external cavities for laser stabilization.

Observation of normal GVD frequency comb

Generation of Kerr frequency comb is phase matched in a broad range of parameters if GVD of the resonator modes is anomalous. However, phase matching is compromised in the case of purely normal GVD. While modulation instability as well as mode locking is still possible under this condition, generation of a broad frequency comb has not been previously demonstrated under net normal GVD.

Short optical pulses can be created in a Kerr frequency comb system if the optical loss of a nonlinear ring microresonator has specific frequency dependence. The loss dependence modifies the GVD of the resonator in a way similar to conventional mode locked lasers that can

operate at any GVD. This method, though, is not easily utilizable for a large variety of the broadband monolithic microresonators.

We observed a stable normal GVD Kerr frequency comb (Fig. *4-16*). The shape of the frequency envelope of the comb differs significantly from the earlier predictions and observations. By demodulating the comb on a fast photodiode and observing the phase noise of the generated RF signal we prove that the frequency harmonics are phase locked. To ensure generality of the phenomenon we performed the experiment at two different wavelengths, 780 nm and 795 nm, using several different resonators and confirmed generation of the mode locked combs with similar properties.

Using numerical simulations, we reproduced the frequency comb envelope and shown that the comb does not correspond to generation of a short optical pulse in the resonator; rather, the pulses are "dark," i.e. they have lower power as compared to the DC background in the resonator (Fig. *4-17*). The frequency comb produces bright pulses at the resonator output, due to the interference with the pump light. It is worth noting that generation of bright pulses inside the resonator usually leads to generation of "dark" pulses at the resonator output. The pump light has to be filtered out to enable observation of the bright pulses.
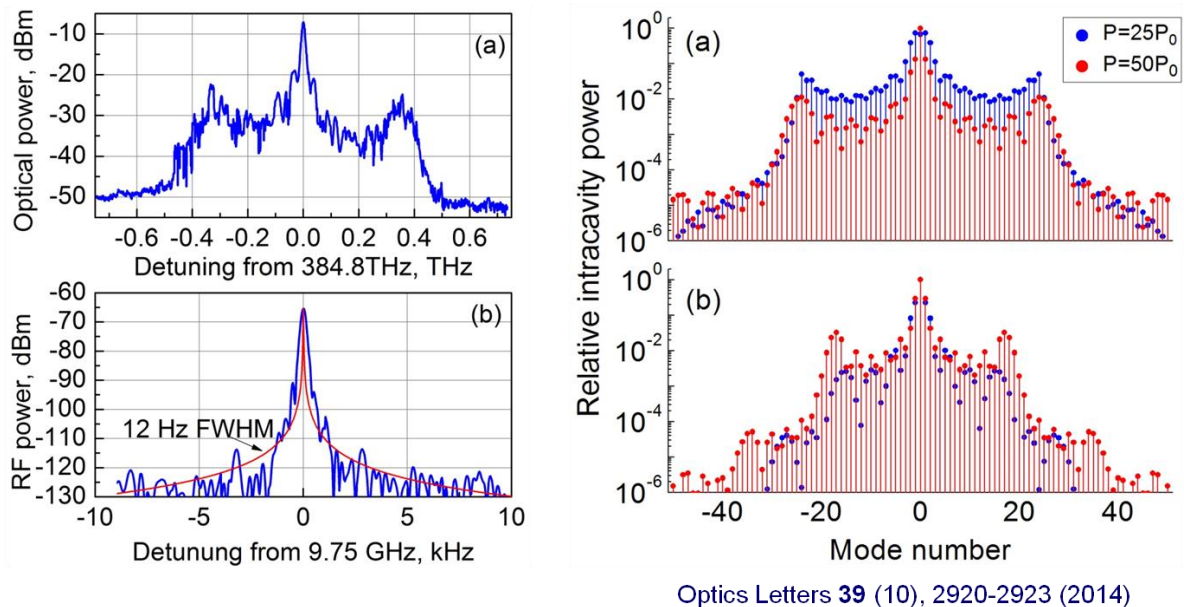
Optics Letters **39** (10), 2920-2923 (2014)

4-16 Left: (a) Observation of Kerr frequency comb at 795 nm in MgF2 resonator. The comb is generated at the conditions of normal GVD. The optical spectrum is not resolved by the spectrum analyzer we used. (b) Spectrum of an RF signal generated by the frequency comb on a fast photodiode. Right: Theoretical simulation of the comb generation. The simulations are performed for various experimental conditions.
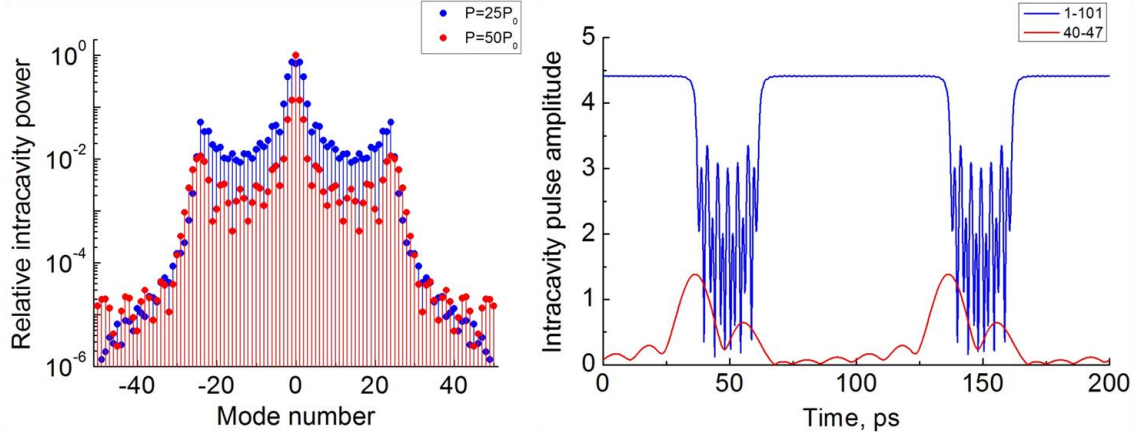
4-17 Left: Normal GVD Kerr frequency combs generated in a WGM resonator for two different values of pump power P. Right: Optical pulses generated in the resonator for pump power P=25P₀ (P₀ is characteristic power of the process described in the corresponding paper). Blue line corresponds to the whole comb spectrum. Red line corresponds to the pulses generated by beating several modes of the comb only.

The first complete analytical study of mode locked Kerr frequency comb

We analyzed mode locked regime of Kerr frequency comb using Lugiato-Lefever (LL) equation accompanied by the standard high finesse cavity input-output equation:

$$T_R \frac{\partial A}{\partial T} + \frac{i}{2}\beta_{2\Sigma}\frac{\partial^2 A}{\partial t^2} - i\gamma_\Sigma |A|^2 A = -\left(\alpha_\Sigma + \frac{T_c}{2} + i\delta_0\right)A + i\sqrt{T_c P_{in}}\,e^{i\varphi_{in}},$$

$$A_{out} = \sqrt{P_{in}}\,e^{i\varphi_{in}} + i\sqrt{T_c}\,A;$$

Here $A(T, t)$ is the slowly varying envelope of the electric field, $T = z/V_g$, z is the is distance traveled by the photon around the resonator circumference (T is "slow time"), $V_g = 1/\beta_1$ is the group velocity, and t is the retarded time (the time in the frame of reference travelling along with the pulse with the group velocity, $t \equiv t* - z/Vg$, where $t*$ is the physical time). T_R is the resonator round trip time, $\beta_{2\Sigma}=2\pi R\beta_2$ is the GVD of the resonator, $\gamma_\Sigma=2\pi R\gamma$ is the nonlinearity of the resonator, α_Σ is the amplitude attenuation per round trip, T_c is power loss per round trip due to coupling, d_0 is the normalized frequency detuning, $\delta_0 = (\omega_0-\omega)T_R$ is the detuning between the pump light and the pumped mode, ω_0 is the eigenfrequency of the optically pumped mode, ω is the carrier frequency of the pumping light, $P_{in}^{1/2}\exp(i\phi_{in})$ stands for the external pump.

We assumed that solution can be found in form

$$A(T,t) = A_c + A_p(T,t),$$

$$A_c = \sqrt{P_c}\,e^{i\varphi_c},$$

$$A_p(T,t) = \sqrt{\frac{P_p}{2}}\left[\sec h\left(\frac{t-\xi}{\tau}\right)\right]^{1+iq} e^{i\Omega(t-\xi)+i\varphi_p}$$

and found parameters of the solution using perturbed Lagrange equations derived from Lagrange operator

$$L = \int_{-\infty}^{\infty} \left\{ \frac{T_R}{2} \left(A_p^* \frac{\partial A_p}{\partial T} - A_p \frac{\partial A_p^*}{\partial T} \right) - \frac{i}{2} \left(\beta_{2\Sigma} \left| \frac{\partial A_p}{\partial t} \right|^2 + \gamma_\Sigma |A_p|^4 \right) \right\} dt$$

Steady state solution as well as timing jitter of the pulse train generated in the resonator was found. The results were published in Optics Express 21 (23), 28862-28876 (2013).

The first demonstration of a diamond microsphere WGM resonator

Diamond is an excellent optical material that is transparent in mid-IR. The material is also attractive because of its exceptional physical and chemical properties, including thermal conductivity, as well as mechanical hardness. Recently developed methods of mass fabrication of inexpensive clean diamond crystals resulted in explosive growth of all kinds of devices based on the diamond. Optical microring resonators have been fabricated out of diamond. It was not clear if the measured Q-factors of microrings are related to the cleanness of the material, or if is limited by the fabrication technique.

Mechanical polishing allows reaching outstanding surface quality that has already led to demonstration of the highest finesse monolithic resonators. We used this technique to fabricate a diamond resonator (Fig. *4-18*). The measured quality factor of the resonator was Q = 2.4x10^7, which is two orders of magnitude larger compared with the best previously reported values. We found that in our case the measured Q-factor is limited by the material loss, which approaches 4 x10^{-3} cm^{-1}, and not by surface scattering.
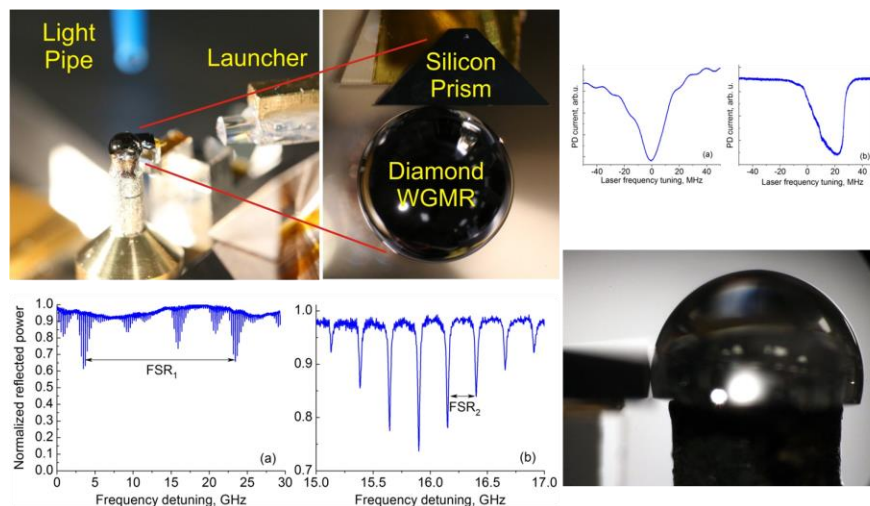
4-18 Demonstration of the first diamond WGM resonator: setup and optical spectra.

Mid-IR Optics

Experimental setup for the Kerr comb generation in the mid-IR

Considerable interest surrounds the generation of Kerr combs at mid-IR wavelengths, which may enable innovative molecular fingerprinting applications for in-situ and remote

biochemical detection. To date, however, the pursuit of this objective has been generally hampered by the lack of a viable approach to pumping microresonators at mid-IR wavelengths (for example, evanescent coupling from tapered fiber is not an option due to high mid-IR loss in fused-silica fibers), lack of suitable pump laser, and/or high mid-IR loss in the resonator material itself.
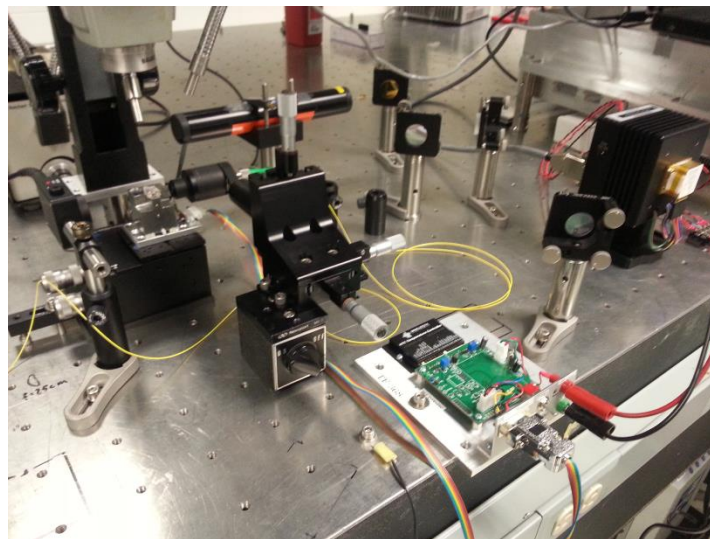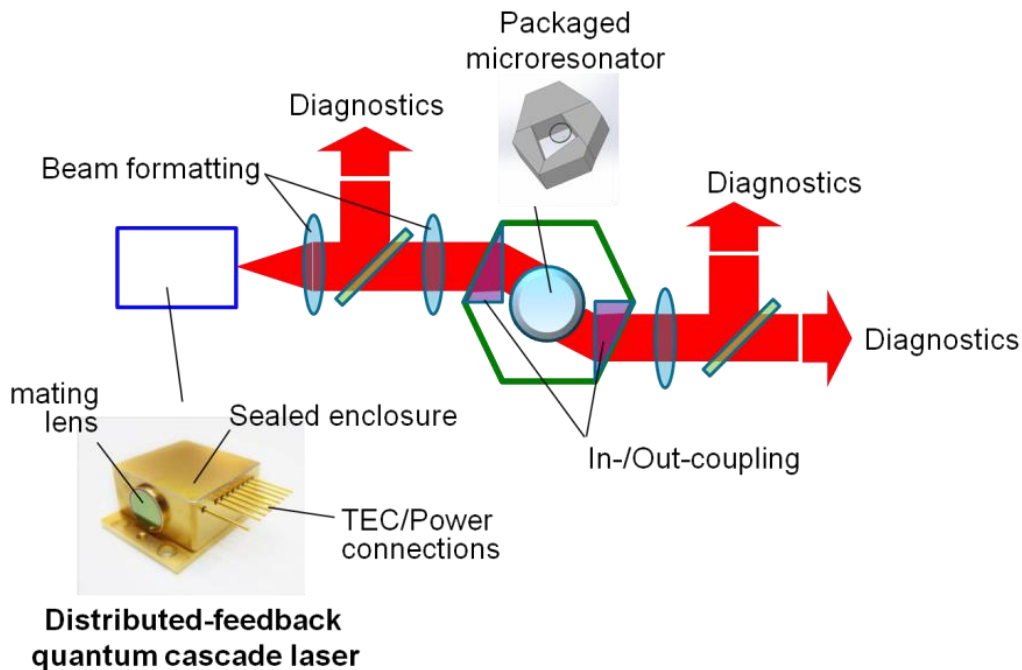
4-19 Up: Schematic view of experimental setup for mid-IR Kerr comb generation.
Down: Photograph of the experimental setup at Aerospace.

We pursued an experimental realization of a mid-IR Kerr comb, which circumvents these issues, as illustrated in Fig. *4-19*. In our experiment, the pump laser was distributed-feedback (DFB) QCL operating at central wavelength of approximately 4.51μm. We acquired the laser as

an off-the-shelf item from Adtech Optics and performed its characterization at Aerospace laboratory facilities, as documented in Fig. 4-20.

The DFB QCL emits maximum CW output power in excess of 75mW, exhibits single-frequency spectrum (supplier-specified linewidth < 1 MHz) which can be continuously temperature-tuned, without mode hopping, over a wavelength range >10nm, and emits a single-transverse-mode near-Gaussian beam of excellent spatial quality ($M^2 \sim 1.2$).

We coupled the output beam from the QCL into the packaged microresonator (which was transported from OEwaves to Aerospace facilities). The formatted beam was injected into the resonator using a free-space approach that leverages the mid-IR transparent, prismatic sapphire windows used to enclose the microresonator. This approach avoids the optical loss that would be incurred by using, for example, silica fibers (opaque at wavelengths > 2.7µm) for light transport. A single-frequency 1.5µm fiber laser (NKT-Photonics/Koheras Adjustik) is also included in the setup to provide a pilot beam to guide the alignment process.
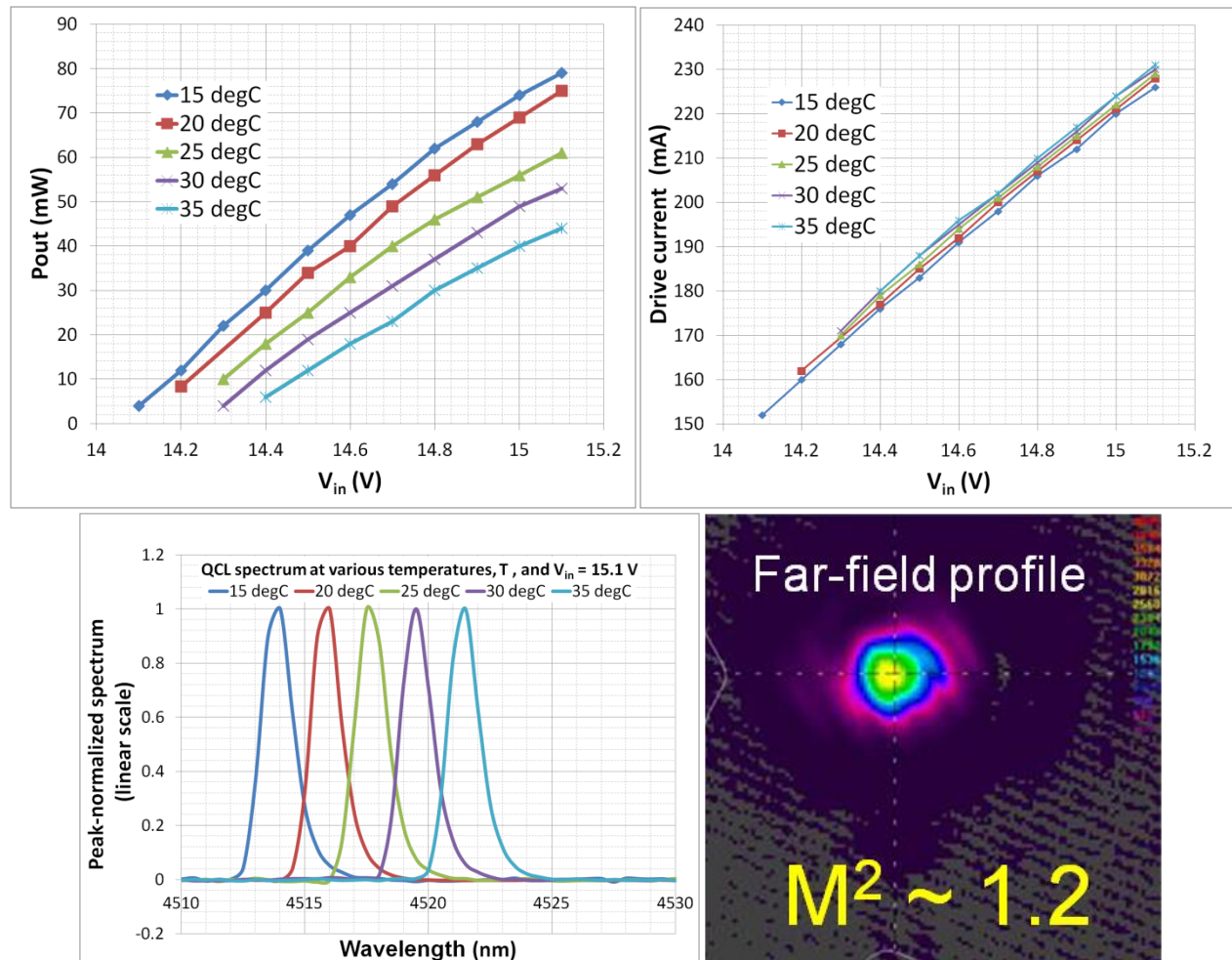
4-20 *In clockwise direction from top:* *QCL output power vs. DC voltage across diode leads for various QCL temperature values; QCL drive current vs. applied DC voltage; Far-field spatial profile of the QCL output beam at max power; QCL output spectrum recorded with a monochromator for several temperature values (the spectral width is instrument-limited).*

Resonator package

We designed a packaged resonator that is protected from environmental contamination to study properties of the generated frequency comb as well as the properties of the self-injection locked laser emission.

Design of resonator package

High-Q WGM resonators are prone to degradation under such environmental factors as dust and humidity. A proper package should be designed to make a resonator suitable for transportation outside the clean room environment. The package must also provide low thermal sensitivity. The distance between the evanescent field coupler surface and the resonator circumference is on the order of 0.1 um. Thermal changes of the package should not lead to closing the gap between the resonator and the coupling prism; otherwise the prism will damage the resonator.

We designed a sapphire package shown in Fig. *4-21*. The walls of the box are used to couple light in and out of the resonator. The box is designed such that the resonator can be operational in a laboratory environment and outside the clean room.
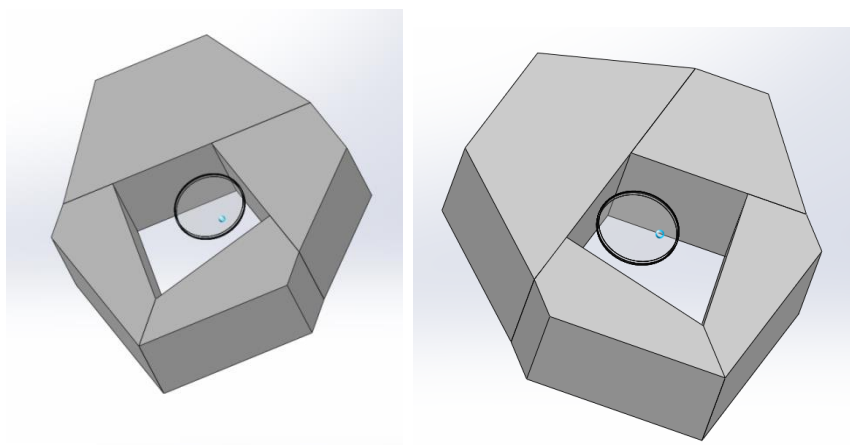
4-21 Design of sapphire box for the resonator. The walls of the box are used as the coupling prisms.

We reviewed properties of several materials transparent in the mid-IR and found that sapphire is the most suitable for fabrication of couplers for WGM resonators made either from calcium or magnesium fluoride (*Table 1*). The basic advantages of sapphire are transparency in the visible and near infrared, as well as high mechanical quality.

Table 1: Indexes of refraction for several optical materials transparent at 4.6 um.

Prism material	Refractive index at 4.6 um
BaF_2 (partially soluble in water)	1.455
Sapphire	1.652
Zink Selenide	2.435
Silicon	3.43
GaAs	3.14
Spinel (MgAl2O4)	1.71

Diamond	2.38
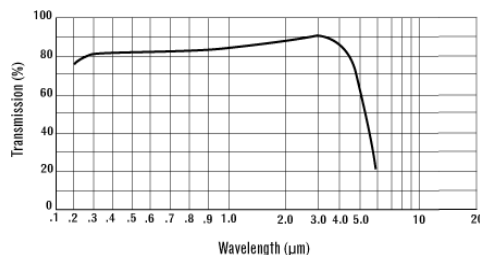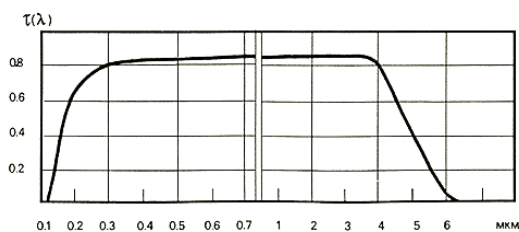
Refractive index of sapphire allows coupling with resonators made out of quartz, fused silica, various fluorides, since the index of refraction of sapphire is large enough (see Fig.*4-22* and *Table 2*). On the other hand, it is not as large as refractive index of silicone or germanium, so the boundary reflection is not very large.

Table 2: Wavelength dependence of refractive index of sapphire.

Sapphire refractive index for ordinary ray

Wavelength, mkm	0.3	0.4	0.7	1.0	2.0	3.0	4.0	5.0
Refractive index	1.814	1.785	1.763	1.757	1.740	1.713	1.677	1.623

We mounted the sapphire box at a thermally stabilized platform and verified thermal stability of the platform using commercial simulators (Fig.*4-23*).
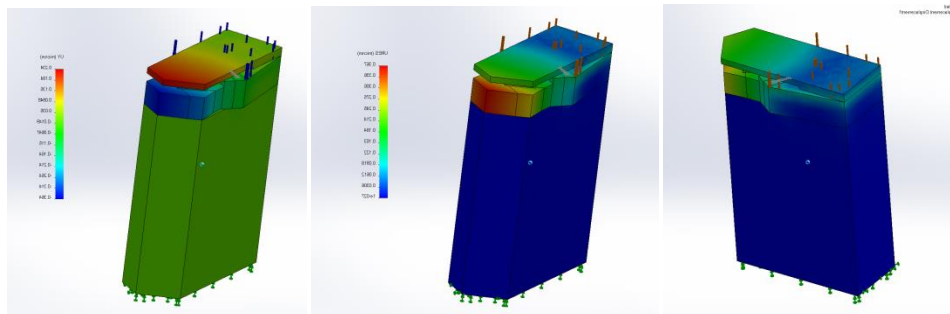
4-23 Example of simulations of thermo-mechanical properties of the sapphire package designed for the resonator. We insured by the simulations that reasonable temperature change does not result in significant deformation of the package.

<u>Assembly of resonator package</u>

We fabricated parts and assembled the packaged resonator in accordance with the design. The picture of the package is shown in Figure 4-24. To verify the quality of the resonator we checked the quality of the optical beam leaving the resonator (Figure *4-25*) and the full width at the half maximum of the resonator (Figure *4-25*).
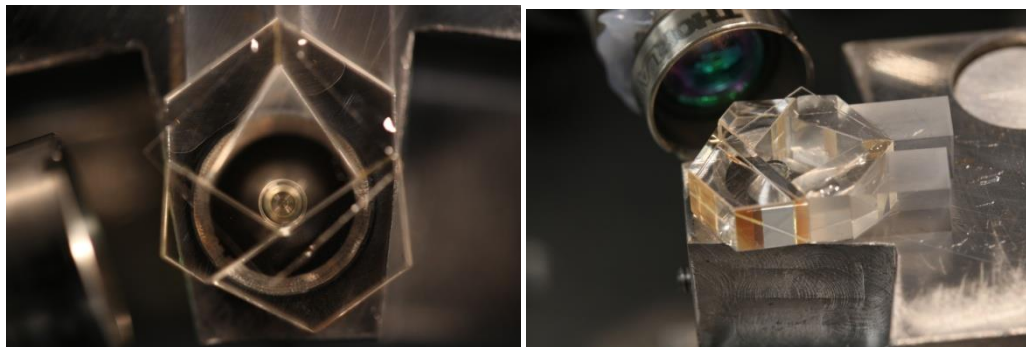
4-24 *Packaged MgF$_2$ microresonator in accordance with the design shown in Figures 4-23 and 4-21. The space gap between the prism and the resonator surfaces is fixed at about 200 nm*

Both measurements were performed at OEwaves using a 1.5 um laser. The measurement is possible since sapphire is transparent at 1.5 um and 4.6 um. The measured FWHM is optimal for the generation of the fundamental Kerr frequency comb, in accordance with the results of GVD simulations presented in Table 3 below. The packaged resonator was transferred to Aerospace Corp. for further study.
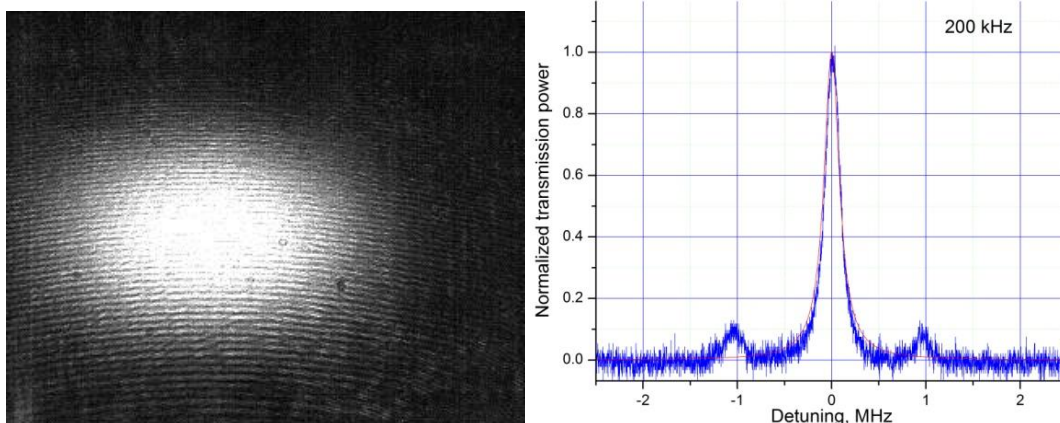
4-25 *Left: Far field picture of the light exiting the resonator at 1,500 nm. The picture confirms good beam quality. Right: Full width at the half maximum for the packaged resonator measured at ~1550 nm wavelength.*

Coupling of mid-IR coherent emission of a QCL to the packaged whispering gallery modes of the resonator was achieved and recorded. To prove that the coupling was achieved we measured both reflected and transmitted light through the resonator. Both signals were recorded (see Fig. *4-26* and Fig. *4-27*), which means that we succeeded in coupling light to a WGM.

First evidence of QCL coupling to microresonator

Reflected beam   Transmitted beam
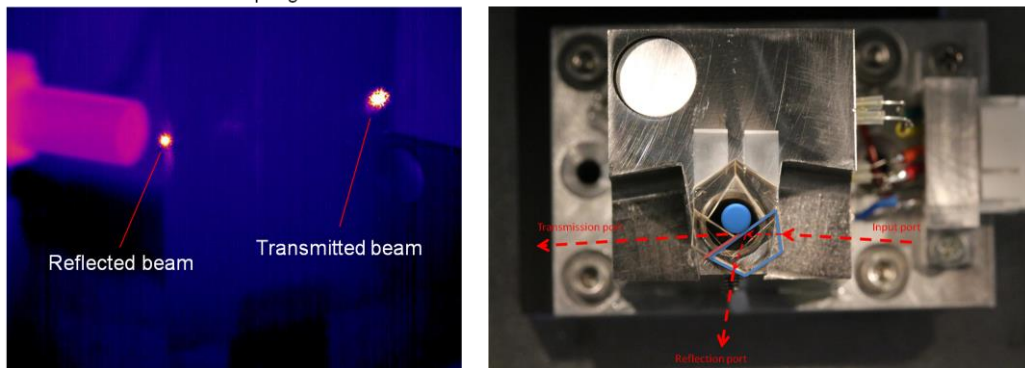
4-26: Left: Picture of reflected and transmitted mid-IR beams made using a mid-IR camera. Right: Schematic of the experiment.

Unfortunately, the resonator was damaged/contaminated during the experiments, so no Kerr frequency comb was observed. The resonator Q-factor dropped by several orders of magnitude in a couple of months. The contamination likely came from humidity in the lab and resulted in oxidation of the resonator package (see inset in Fig. *4-27*). The package was not hermetically sealed at that time. We came to the following conclusions as the result of the experiment:

- Measured bandwidth was reduced to 300-400MHz from sub-MHz.
- There was no thermal nonlinearity or thermo-refractive noise observed at any laser power. This observation also indirectly shows that Q is too small to produce any other nonlinear effect.
- The spectral cleanness and analysis of the far field with photodiode suggested good mode matching.
- It was impossible to inspect the air-gaps
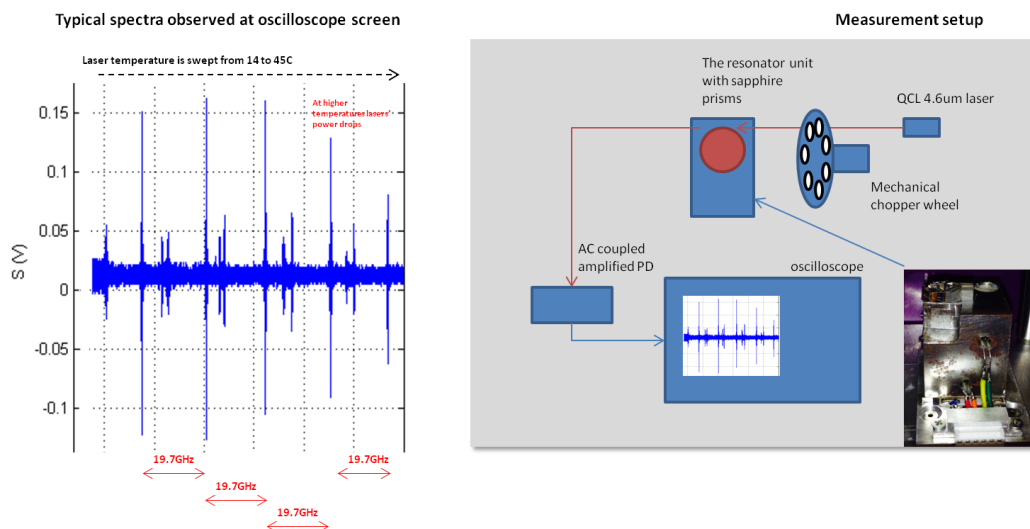
4-27: Left: Spectrum of the resonator. Right: Measurement setup. Inset: Picture of the resonator package with excessive oxidation of the steel pedestal.

We decided to i) improve the package and cover it with hermetic cover to reduce the damage probability; ii) create a self-injection locked QCL that can be used for comb generation and also for alignment and quality control of the packaged WGM resonator to be deliver to the Aerospace Corp. for further experiments. Since the establishment of these objectives, <u>we have demonstrated the first mid-IR Kerr frequency comb,</u> as it was planned in Year II of the effort.
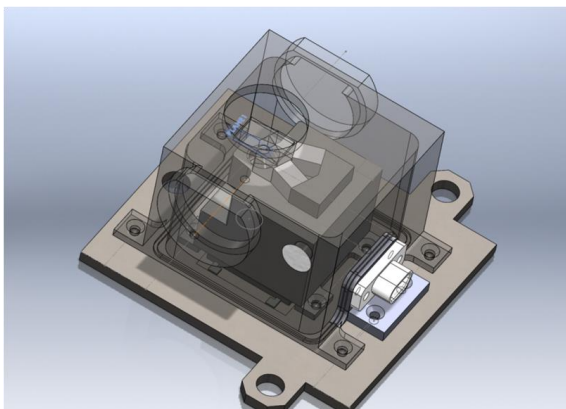
4-28: A new design of a MgF2 WGM with hermetically sealed package.

We designed, fabricated, and packaged a new magnesium-fluoride (MgF_2) microresonator suitable for generation of mid-infrared frequency combs. The package was improved significantly and protected from environment (Figure *4-28*). The packaged microresonator was delivered to the Aerospace Corp., for experiments to couple light emitted by a single-transverse-mode, single-frequency distributed-feedback quantum cascade laser (QCL) operating at 4.5 μm wavelength into the microresonator. The effort was aimed at demonstrating the first microresonator-based Kerr comb at mid-infrared wavelengths.

The first demonstration of a self-injection locked QCL

In this effort we also designed and built the first self-injection locked QCL. To make the device we procured an AdTech QCL mounted on a C-mount. The laser was integrated with a CaF2 WGM resonator having 10 GHz free spectral range. The output of the self-injection locked laser was coupled to a single mode 4.5 um fiber. The scheme and picture of the device is shown in Fig. *4-29*. The laser has sub-kHz linewidth. The self-injection locked QCL can be made broadly tunable, which will open a new page in mid-IR molecular spectroscopy studies.

4-29: Left: Scheme of the read-board self-injection locked QCL. Right: Picture of the assembled unit.

The first demonstration of the mid-IR Kerr frequency comb

We have studied GVD and absorption of MgF2 and CaF_2 resonators at 4.6 um for a WGM resonator with diameter on the order of 2.7mm (Table 3). The dispersion is large and anomalous, which is optimal for generation of optical frequency combs. The absorption of the material was expected to be small (see Fig. *4-30*). However, the experiment had shown that it is much larger, so Q-factor of the resonator does not exceed 10^8.

Table 3: *Dispersion parameters of magnesium and calcium fluoride resonators calculated at 4.6 um.*

Resonator Material	Refractive index	Dispersion parameter, ~24 GHz FSR	Radius, cm
CaF2	1.404	300 kHz, anomalous	0.1361
MgF2	1.3497 (ne); 1.3404 (no)	526 kHz, anomalous	0.1415 (e)
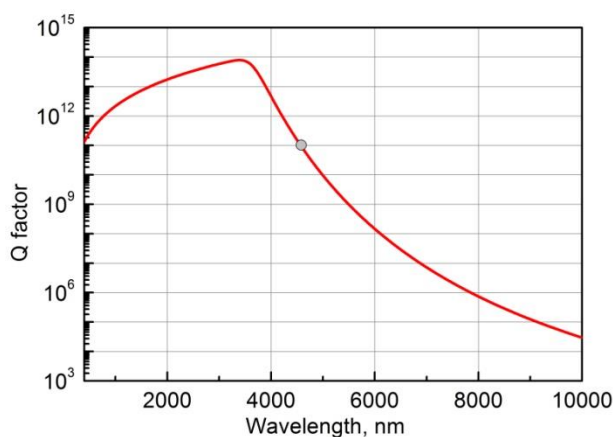
4-30: Calculated theoretically quality factor limit versus wavelength for a calcium fluoride WGM resonator. The calculations are based on available measurement data for the material transparency in the UV, VIS, and IR frequency ranges. The maximum Q-factor exceeds 100 billion in the vicinity of 4.6 um (shown by gray circle). It worth noting that the maximum Q-factor observed at 1550 nm approaches 3x10^{11} and is limited primarily by imperfectness of the material.

We demonstrated generation of a Kerr frequency comb centered at 4.5 um using the self-injection locked laser as early as April 2014. This is the first demonstration of a directly generated Kerr comb at such a long wavelength. The comb was generated when laser power fed to a selected WGM of the resonator exceeded certain threshold.

Snapshots of the comb spectra are shown in Figure *4-31*. The measurements were performed using Thorlabs OSA205, that according to its specs has approximately 7.5 GHz resolution at 4.5 micron wavelength (corresponding to >12GHz 3dB resolution of two spectral harmonics) and -60 dBm noise floor. These specifications are not enough to resolve harmonics of the frequency comb separated by 10 GHz. We were able to observe the comb envelope, only. High order harmonics separated from the pump frequency by hundreds of GHz are clearly seen at Fig. *4-31*.
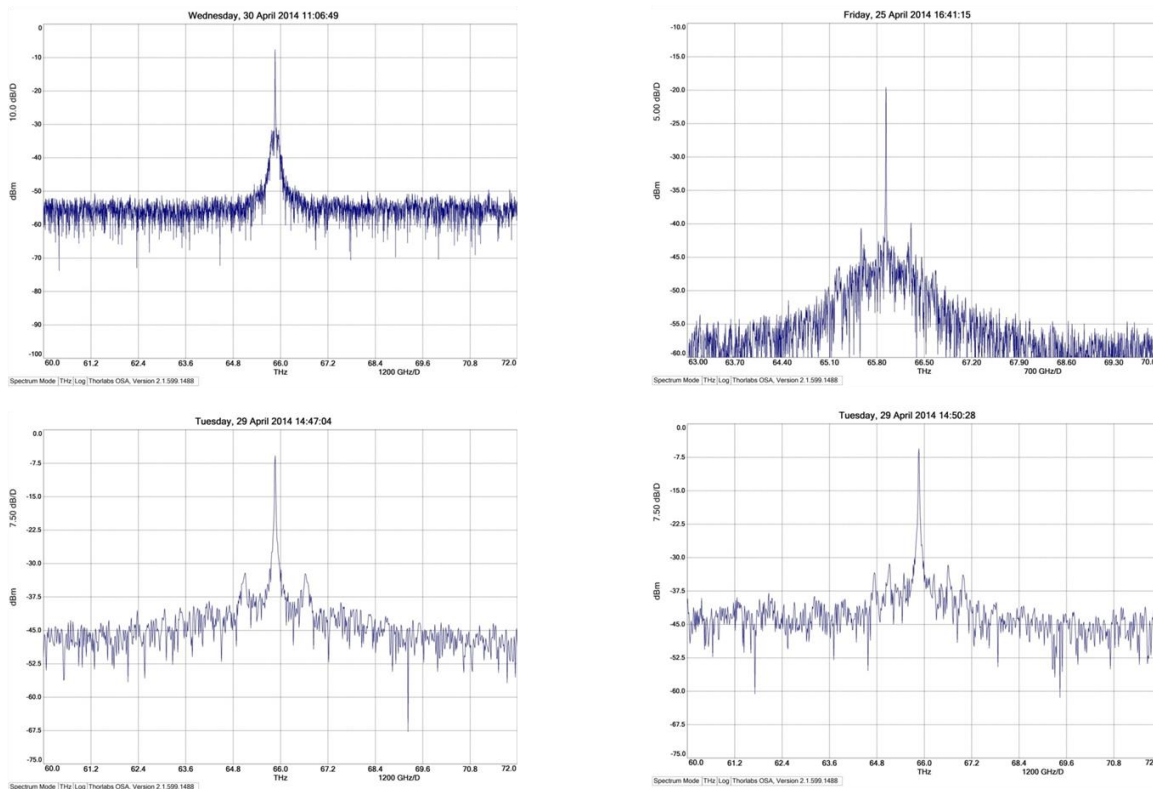
4-31: Examples of the spectra of the Kerr frequency comb generated in the self-injection locked laser-based unit (see Fig. 4-29).

Generation of a broad mid-IR frequency comb: a summary of the mid-IR comb generation effort

In this section we summarize our efforts performed after the initial observation of the mid-IR frequency comb. We first describe why the problem is important, then list known approaches to generate mid-IR combs, and present our results. The main results of the effort are presented in this section.

Optical frequency combs represent an invaluable tool for atomic and molecular spectroscopy by providing the means for precise spectral calibration and parallel interrogation of multiple absorption features over a wide range of wavelengths [1-6]. Comb generation in the mid-infrared (mid-IR) is especially attractive as it permits access to the molecular "fingerprint" region of the optical spectrum (~3-20μm wavelength), which contains strong ro-vibrational absorption features for many chemical species of environmental, industrial, medical, and military interest [7-9].

Direct generation of frequency combs is well established for the near-IR region of the spectrum owing to the availability of mature mode-locked sources such as titanium:sapphire and ytterbium-, erbium-, and thulium-doped fiber lasers [10-12]. As mode-locked laser technology is far less advanced at longer wavelengths [13-15], mid-IR frequency combs have often been obtained via parametric down-conversion of near-IR lasers in nonlinear crystals, which typically results in complex, laboratory-bound optical systems [16-23]. For field applications and insertion

Contract No:
FA9550-12-C-0068   OEwaves, Inc.   27

into portable instruments, more compact and rugged architectures are desirable. In principle, quantum cascade lasers (QCLs) would represent ideal sources for such architectures owing to their broad spectral coverage in the mid-IR ($>3.5\mu m$), excellent beam quality, room-temperature operation, high electro-optic efficiency, and inherent support for "on-chip" integration [24-27]. Recently, a specially designed, $\sim7\mu m$ wavelength QCL was mode-locked to generate a $\sim1\mu m$-wide comb [28, 29]. However, standard commercially available QCLs are generally unsuitable for direct comb generation because they exhibit relatively narrow gain bandwidths. They also are inherently difficult to mode-lock because the lifetime of their emitting states is shorter than the laser cavity roundtrip time [30-32].

An alternative approach to generating broadband mid-IR combs within a practical and miniaturizable platform is to use a continuous-wave (CW) QCL to optically pump a whispering-gallery-mode (WGM) microresonator [33-38]. In these devices, frequency combs (also referred to as Kerr combs) can be generated via cascaded four-wave mixing (FWM) processes initiated by frequency locking an external, "pump" laser source to a resonator WGM. Such cascade FWM processes, also known as "hyper-parametric oscillation", are often driven by modulation instability [39] and result in the emission of a spectrally broad set of sidebands spaced by one or multiple free-spectral ranges of the resonator [40, 41]. Sidebands can be efficiently produced, even for mW-power CW pump sources, owing to the very tight optical confinement and very high quality factor (Q) of the WGM microresonator, which greatly enhance the photon density within the resonator modes, leading to strong nonlinear light/matter interactions (the Kerr effect) [42].

To date, nearly all realizations of Kerr combs have been near-IR pump lasers (*e.g.* ~ 1 or 1.5 μm diode lasers) and have not extended beyond ~ 2.5 μm [43]. Very recently, a Kerr comb generated in a silicon micro-ring was reported to reach ~ 3.5 μm [44]. However, attaining even longer wavelengths would be highly beneficial. For example, light in the 4-5μm wavelength range exhibits good transmission through the atmosphere and overlaps with strong absorption bands of important greenhouse gases such as carbon dioxide ($\sim4.2\mu m$) and nitrous oxide ($\sim4.4\mu m$), carbon monoxide ($\sim4.6\mu m$) and carbonyl sulfide ($\sim4.8\mu m$).

In this Project we demonstrated the feasibility of combining QCLs and crystalline WGM microresonators to produce mid-IR Kerr combs within compactly integrated platforms. As our pump QCLs operated at 4.5μm, the Kerr combs were generated at the longest wavelengths observed to date.

We selected magnesium- and calcium-fluoride (MgF_2 and CaF_2) as the host materials for the fabrication of crystalline microresonators, mainly because of their excellent optical transmission in the mid-IR, which affords very high Q values, and anomalous group-velocity dispersion (GVD) at 4.5 μm. The anomalous GVD helps reduce the threshold power for the onset of hyper-parametric oscillation and effectively favors FWM and comb generation over parasitic nonlinearities such as Raman scattering [34, 45, 46].
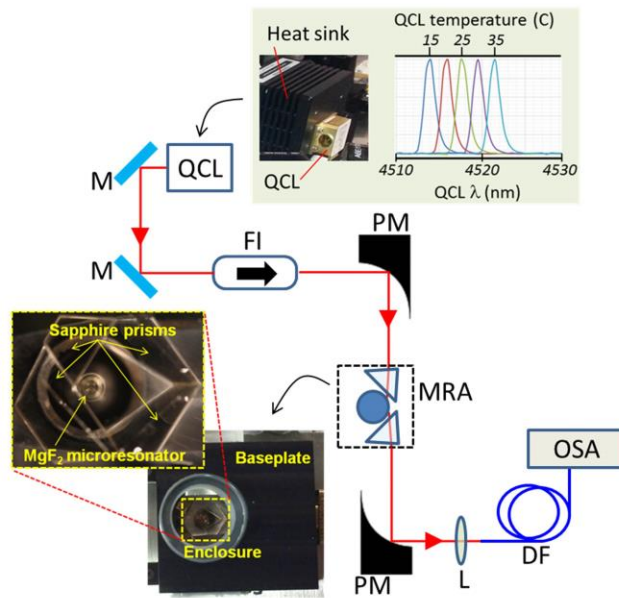
4-32: QCL: Distributed-feedback, ~4.5μm-wavelength quantum cascade laser (inset: photograph of the laser enclosure, temperature-tuning properties, and far-field profile of the laser output beam); M: Beam-steering mirror; FI: Faraday isolator; PM: Off-axis parabolic mirror; MRA: Microresonator assembly (inset: top-view photographs of the resonator and its sapphire-prism enclosure); L: Lens; DF: Single-mode delivery fiber; OSA: Optical spectrum analyzer.

In our first experiment, we used a commercially available, distributed-feedback (DFB) QCL emitting a single-frequency, near diffraction-limited Gaussian beam with a 4.5μm central-wavelength, and up to ~60mW CW power, to optically pump an MgF_2 crystalline microresonator (see Fig. *4-32*). The microresonator was shaped as a truncated oblate spheroid of 1.8 and 0.25 mm semi-axis dimensions and approximately 0.5 mm thickness [46]. The resonator intrinsic Q factor at ~ 4.5 μm was ~2×10^8, corresponding to ~330 kHz bandwidth. The QCL output beam was collimated and evanescent-field coupled [47] into and out of the microresonator by means of sapphire prisms. The microresonator was installed in a protective enclosure, which provided temperature control to within 10^{-3} K. The temperature control and judicious use of materials having dissimilar thermal expansion coefficients for resonator, coupling prism, and mounting substrate, enabled the fine adjustment of the resonator/coupling-prism air gap dimension to within ~100nm. The QCL output beam was passively coupled to microresonator WGMs via thermal frequency locking, made possible by the positive thermo-optic (dn/dT) coefficient of MgF_2 [40, 48].

Kerr combs could be generated for QCL output powers as low as ~ 2 mW, when the prism/resonator gap was adjusted to yield a loaded resonator Q factor of ~ 1.5×10^8 (~ 450 kHz bandwidth). We observed two distinct combs characterized by mode spacing of ~ 2100 and ~500 GHz (Fig. *4-33*), respectively, which could be generated at smaller and larger offsets of the QCL laser frequency relative to the WGM mode frequency. As the QCL power was increased to ~55 mW, the wider-spaced Kerr comb stretched to more than half of an octave (~3.7 to ~5.5 μm, corresponding to over 25 THz), while the narrow-spaced comb remained confined to a ~ 2.5 THz region around the pump wavelength (Fig. *4-33*b).
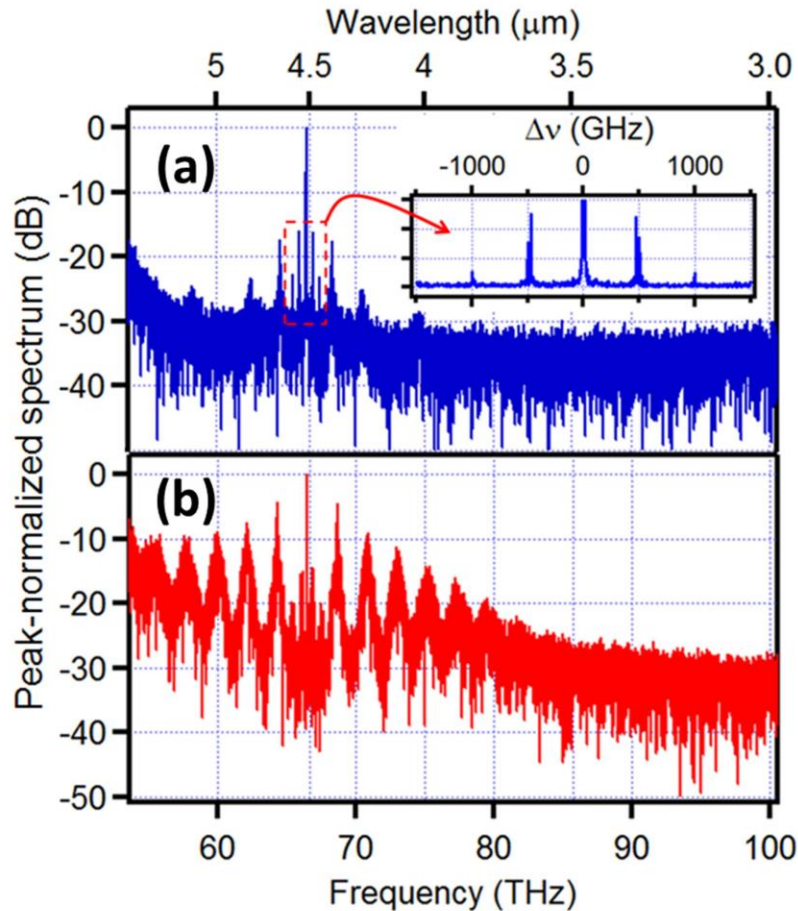
4-33: *Logarithmic-scale, peak-normalized spectra of Kerr combs, obtained by optically pumping the MgF2 microresonator with ~55mW power at ~4.5 μm wavelength. The spectra in (a) and (b) were obtained for different values of detuning between the pump laser frequency and resonator modes. A narrow-spaced (~500 GHz) comb, spectrally localized in the vicinity of the pump, persisted for a relatively wide range of detunings. A linear-scale spectrum of this comb plotted vs. frequency difference from the pump is shown in the inset of (a). A more widely spaced (~2.1 THz) comb, shown in (b), could be obtained for a narrower range of detunigs and spanned half an octave.*

To illustrate the potential for compact and robust packaging of QCL-pumped WGM microresonators, we designed and built a demonstrator device consisting of a 4.5μm-wavelength DFB QCL chip, silicon collimating lenses, barium fluoride (BaF_2) prism coupler, and truncated-spheroid microresonator (3 and 0.21 mm semi-axis dimensions, ~0.5mm thickness), all mounted on a thermo-controller base (see Fig. *4-34*). For this device, the microresonator host material was calcium fluoride (CaF_2), which shares many relevant optical and mechanical properties of MgF_2. The device concept and overall dimensions (approximately 75×50×10 mm) are similar to those of previously reported units, in which we integrated WGM microresonators and ~1.5μm-wavelength telecom-type DFB diode lasers [49]. Because the negative thermo-optic coefficient of CaF_2 makes thermal locking impractical, coupling of the QCL output to select WGMs of the microresonator was obtained by self-injection locking [49]. This approach also allows a robust and compact packaging of the laser-resonator system.
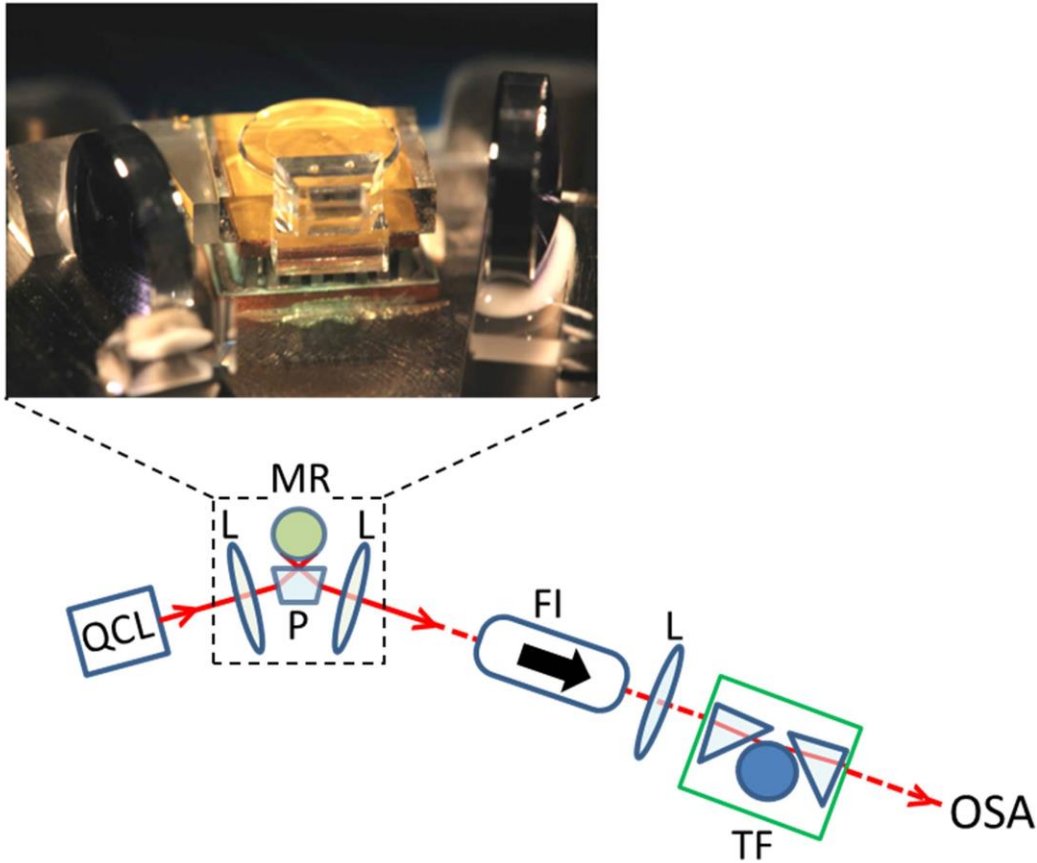
4-34: QCL: Distributed-feedback, ~4.5µm-wavelength quantum cascade laser; L: Lens; P: Evanescent-field coupling prism, MR: Microresonator (inset: photograph of the compactly packaged resonator/coupling-prism/coupling-lens assembly); FI: Faraday isolator; TF: Tunable Lorentzian filter consisting of a second, MgF2 microresonator equipped with evanescent-field coupling prisms and installed on temperature-controlled base; OSA: Optical spectrum analyzer.

In the CaF_2 device we observed the generation of a Kerr comb at pump power as low as ~ 15 mW. As we maximized the QCL power within the resonator to ~30mW, the comb stretched to a width of approximately 10 THz (Fig. *4-35*). Similar to the case of the MgF_2 microresonator, we could obtain different Kerr comb line spacing for different values of the QCL frequency to WGM offset. Moreover, for both resonators, the amplitude profiles of the comb envelopes, as well as the overall process of comb formation, appeared very similar to Kerr comb generation regimes driven by the modulation instability usually observed and analyzed in fused silica microresonators pumped at ~1.5µm [50]. We characterized the observed spectrum by fitting comb lines to a Lorentzian profile (see Fig. *4-36*), which yielded a 3dB linewidth ~ 60 kHz, *i.e.* over an order of magnitude narrower than the linewidth of the free-running QCL (~3 MHz).

In conclusion, we have demonstrated the generation of the longest-wavelength Kerr combs to date by optical pumping of crystalline WGM microresonators with 4.5µm-wavelegnth DFB QCLs. The combs were observed for both thermal and self-injection passive locking of the QCL frequency to that of the resonator modes, and the comb width could exceed half an octave. Our experiments show that the generation of long-wavelength mid-IR combs can be obtained by combining QCLs and fluoride microresonators within integrated compact platforms in a manner

similar to well-established near-IR systems that are based, for example, on telecom-type diode lasers and silica resonators.
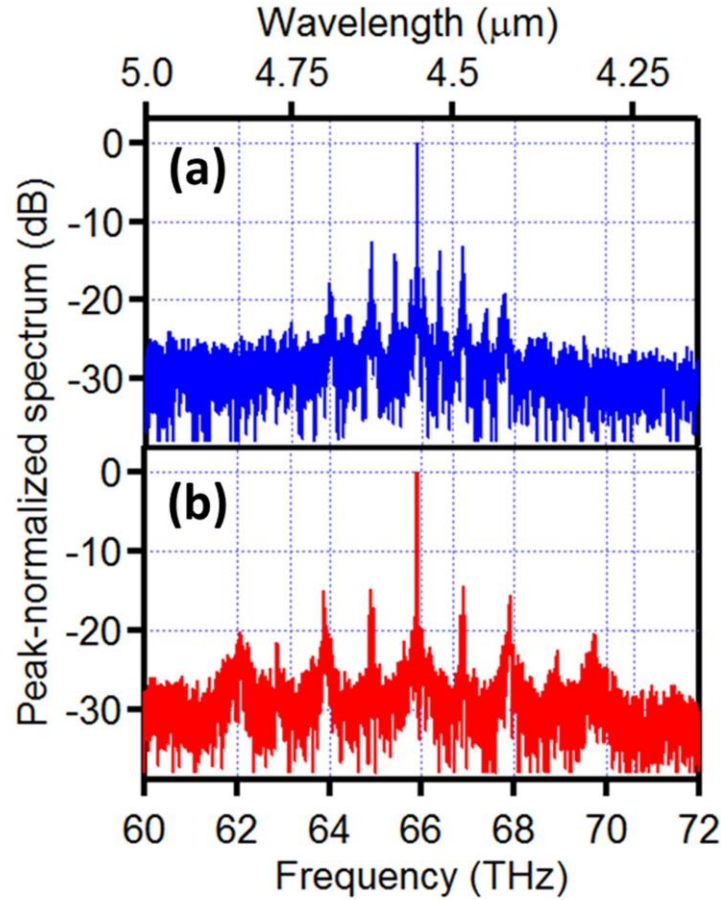
4-35: (a) Logarithmic-scale, peak-normalized spectrum of Kerr comb obtained by optically pumping the CaF2 microresonator with ~30mW power emitted by a ~4.5μm wavelength, distributed-feedback quantum cascade laser (QCL) self-injection-locked to a resonator WGM. (b) Kerr comb spectrum obtained for the same pump power, but with different QCL/resonator-mode frequency detuning.

Methods
Microresonator fabrication and properties
Both microresonators described in this article were fabricated by cutting MgF_2 and CaF_2 cylindrical preforms disks and successively fine polishing their circumferential edge into a spheroidal profile [51]. This resonator morphology has been shown to yield anomalous GVD.
The GVD value can be conveniently characterized by the dimensionless parameter D, defined as [39, 40]

$$D = \frac{1}{\gamma_i}(\nu_{i-1} + \nu_{i+1} - 2\nu_i) = -2\pi c \frac{\beta_2(\nu_i)\nu_{FSR}^2}{n_i\gamma_i}.$$

Here, "i" is a mode number, ν_i (γ_i) is the optical frequency (half width at half-maximum) of the ith resonator WGM, n_i is the refractive index of the host material corresponding to the frequency ν_i, c is the speed of light in vacuum, and $\nu_{FSR} = (\nu_{i-1} + \nu_{i-1})/2$ is the free spectral range (FSR)

Contract No:
FA9550-12-C-0068

of the resonator, and β_2 is the GVD of the resonator host material. Based on the known material dispersion and morphology of the resonators and assuming $\gamma_i \sim 170$ kHz, we obtain $\nu_{FSR} \sim 19.3$ and 11.2 GHz, hence D ~ 2 and 0.35 for the MgF_2 and CaF_2 resonators, respectively. The estimated D values are very suitable for the generation of stable, mode-locked Kerr combs and are known to enable observation of a diverse variety of comb structures including hyper-parametric oscillations, type-II combs, and Turing patterns, which can all be accessed by judiciously adjusting the detuning between the pump laser optical frequency and WGM spectrum [39, 52-54]. Smaller values of D can result in broader comb generation for a given pump power and resonator Q, although the number of possible comb regimes would increase, which may degrade stability [41].

Both resonators had Q factors exceeding 10^{10} at ~ 1550 nm. The value of Q degraded by approximately two orders of magnitude in the mid-IR due to more pronounced multi-phonon effects and greater optical absorption by residual organic impurities [55]. As reported above, the MgF_2 resonator intrinsic Q at mid-IR wavelengths was measured to be ~ 2×10^8. This value was obtained by using the analytical expression derived in Ref. 56 to model the measured resonator spectral-line visibility vs. distance between resonator and coupling prism. We did not measure the intrinsic Q value for the CaF_2 resonator used here, since it was monolithically integrated with the QCL; its Q was inferred to be ~ 3×10^7 (corresponding to ~3 MHz bandwidth) based on comparison with other similar resonators available in our laboratory.
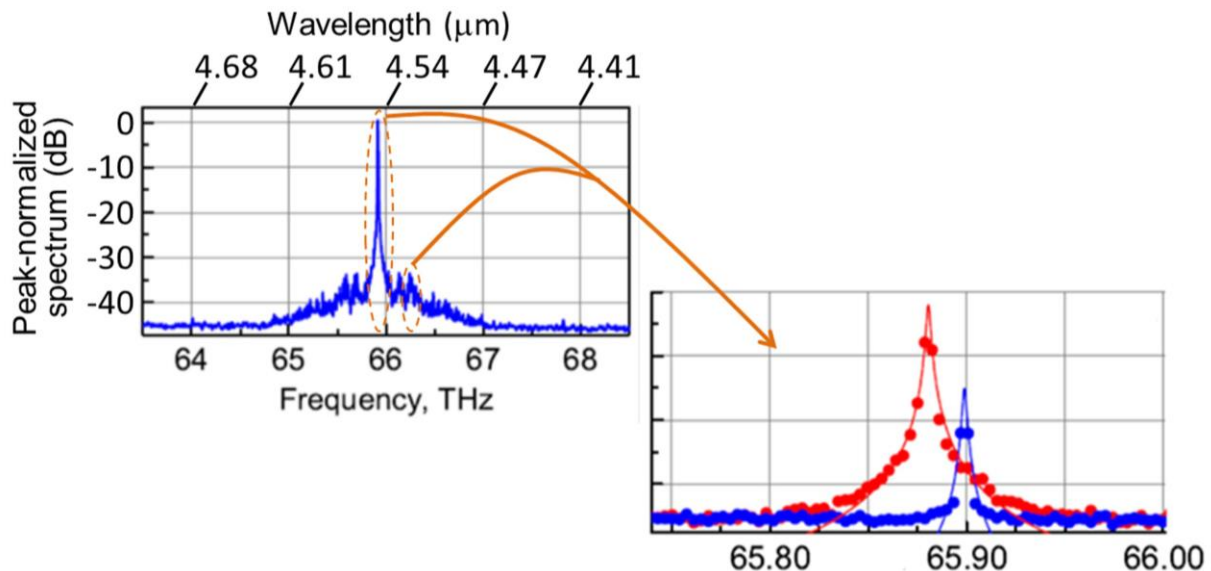
4-36: Lorentzian fit (solid lines) to the pump (red dots) and to a Kerr comb spectral (blue dots) lines observed at the exit of the CaF2 microresonator optically pumped by ~20mW-power, 4.5□m light. The two lines were isolated from the full spectrum by using a separate MgF2 microresonator as a tunable ~4MHz full-width-at-half-maximum (FWHM) band-pass filter. The Lorentzian fit yielded FWHM ~ 60kHz for both lines.

Experimental setup and detection of the spectra
The pump laser used for the MgF_2 resonator experiment was a thermo-electrically cooled, 4.5□m-wavelength DFB QCL (Adtech Optics, "HHL" package), installed within a sealed and nitrogen-purged enclosure that included a collimating lens and zinc selenide exit window. The

QCL emitted a single-transverse-mode near-Gaussian beam having M^2 ~1.2 and was mounted on a commercial heat sink (Arroyo "244-HHL"), which allowed us to temperature-tune the QCL output wavelength, without mode hops, over a >10nm-wide window at tuning rate ~0.37nm/K. The QCL output beam was transmitted through a mid-IR Faraday isolator (Innovation Photonics), then formatted and injected into the microresonator enclosure by a gold-coated off-axis parabolic mirror having 50.8mm reflected focal length. A similar parabolic mirror was used to collect the beam exiting the microresonator. As the optical isolator blocks back reflections from the microresonator, thermal locking only was used to couple the QCL to resonator WGMs. To achieve thermal locking, we varied the driving QCL voltage, thus finely sweeping its output frequency around resonator resonances.

As mentioned above, the MgF_2 microresonator was mounted within an optically transparent enclosure to protect it from dust and humidity, and allow transportability and operation in non-clean-room environments (see Fig. 1). In our design, we used evanescent-field coupling prisms to direct light in and out of the resonator. Uncoated sapphire was chosen as the enclosure material by virtue of its environmental stability, excellent optical transmission at mid-IR wavelengths, and refractive index (~1.65 at ~4.5μm), which is high enough to permit optical coupling into MgF_2 (n ~ 1.34), yet low enough to keep Fresnel reflections down to ~6%. An important property of the resonator enclosure is its excellent thermal stability, which permits fine control of the magnitude of the resonator/sapphire-wall gap to within ~100nm, in a standard laboratory environment.

For the CaF_2 resonator experiment, we used a ~4.5 μm-wavelength, conductively cooled DFB QCL chip (Adtech Optics) as the pump source. The laser emits up to ~50 mW output power in a near-diffraction-limited Gaussian beam. Anti-reflection-coated spherical silicon lenses were used to collimate the QCL beam in and out of the resonator. The beam was injected into the resonator through a single, evanescent-field coupling BaF_2 prism (n ~ 1.45 at ~ 4.5 μm). Up to 60% of the QCL output power could be injected into the microresonator. The insertion loss of the combined resonator/prism/coupling-lens subsystem was measured to be < 3dB. The QCL frequency was self-injection locked to resonator WGMs by letting light generated via Rayleigh scattering within the microresonator back into the QCL (no optical isolation is introduced between QCL and microresonator for this purpose).

In both experiments, the spectral data was obtained by directing the resonator output beam into a Fourier-transform optical spectrum analyzer (OSA) (Thorlabs OSA205) equipped with single-mode, mid-IR transmissive input optical fiber (IRflex). The output power was measured with a mercury-cadmium telluride (HgCdTe) photodetector (Thorlabs PDA10JT).

Since the OSA spectral resolution (8 GHz at ~ 4.5 μm) was marginal for measuring the spectral linewidth of individual comb lines and fully discriminating dense combs, we fabricated a third, stand-alone WGM microresonator (host material: MgF_2) of similar design to those described above. By adjusting the spatial separation between the resonator surface and evanescent-field prism coupler, we could vary the resonator bandwidth in the 0.3 to 300 MHz range, thus effectively obtaining a tunable-bandwidth, first-order Lorentzian band-pass filter. By transmitting the CaF_2 resonator output beam through this MgF_2 filter prior to directing it to the OSA, and were able to fit individual comb lines (recorded over an ~ 1ms-long integration time) to Lorentzian profiles, which yielded a half-width at half maximum of ~60kHz.

References

[1]   T. Udem, R. Holzwarth, and T. W. Hänsch, "Optical frequency metrology," Nature **416**, 233-237 (2002).

[2]   T. W. Hänsch, "Nobel Lecture: Passion for precision," Rev. Mod. Phys. **78**, 1297 (2006).

[3]   S. A. Diddams, L. Hollberg, V. Mbele, "Molecular fingerprinting with the resolved modes of a femtosecond laser frequency comb", Nature **445**, p. 627-630 (2006).

[4]   I. Coddington, W. C. Swann, and N. R. Newbury, "Coherent multi-heterodyne spectroscopy using stabilized optical frequency combs," Phys. Rev. Lett. **100**, 013902 (2008).

[5]   T. Steinmetz, T. Wilken, C. Araujo-Hauck, R. Holzwarth, T. W. Hänsch, L. Pasquini, A. Manescau, S. D'Odorico, M. T. Murphy, T. Kentischer, W. Schmidt, and T. Udem, "Laser frequency combs for astronomical observations," Science **321**, 1335-1337 (2008).

[6]   H. S. Margolis, "Spectroscopic applications of femtosecond optical frequency combs," Chem. Soc. Rev. **41**, 5174-5184 (2012).

[7]   A. Schliesser,   N. Picqué, and T. W. Hänsch, "Mid-infrared frequency combs," Nature Photon. **6**, 440–449 (2012).

[8]   P. Maslowski, K. C. Cossel, A. Foltynowicz, and J. Ye, "Cavity-Enhanced Direct Frequency Comb Spectroscopy," in *Cavity-Enhanced Spectroscopy and Sensing*, pp. 271-321 (Springer, Berlin, 2014).

[9]   L. Nugent-Glandorf, F. R. Giorgetta, and S. A. Diddams, "Open-air, broad-bandwidth trace gas sensing with a mid-infrared optical frequency comb," Appl. Phys. B DOI 10.1007/s00340-015-6070-8 (2015).

[10]   M. J. Thorpe, K. D. Moll, R. J. Jones, B. Safdi, and J. Ye, "Broadband cavity ringdown spectroscopy for sensitive and rapid molecular detection," Science **311**, 1595-1599 (2006).

[11]   B. Bernhardt, A. Ozawa, P. Jacquet, M. Jacquey, Y. Kobayashi, T. Udem, R. Holzwarth, G. Guelachvili, T.W. Hänsch, and N. Picque, "Cavity-enhanced dual-comb spectroscopy," Nature Photon. **4**, 55-57 (2010).

[12]   A. M. Zolot, F. R. Giorgetta, E. Baumann, J. W. Nicholson, W. C. Swann, I. Coddington, and N. R. Newbury, "Direct-comb molecular spectroscopy with accurate, resolved comb teeth over 43 THz," Opt. Lett. **37**, 638-640 (2012).

[13]   E. Sorokin, N. Tolstik, K. I. Schaffers, and I. T. Sorokina, "Femtosecond SESAM-mode-locked Cr:ZnS laser," Opt. Express **20**, 28947-28952 (2012).

[14]   M. N. Cizmeciyan, J. W. Kim, S. Bae, B. H. Hong, F. Rotermund, and A. Sennaroglu, "Graphene mode-locked femtosecond Cr:ZnSe laser at 2500 nm," Opt. Lett. **38**, 341-343 (2013).

[15]   I. T. Sorokina, V. D. Dvoyrin, N. Tolstik, and E. Sorokin, "Mid-IR ultrashort pulsed fiber-based lasers," IEEE J. Sel. Top. Quantum Electron. **20**, 0903412 (2014)**.**

[16]   S. M. Foreman, D. J. Jones, and J. Ye, "Flexible and rapidly configurable femtosecond pulse generation in the mid-IR," Opt. Lett. **28**, 370-372 (2003).

[17]   K. A. Tillman, R. R. J. Maier, D. T. Reid, and E. D. McNaghten. "Mid-infrared absorption spectroscopy acrossa 14.4 THz spectral range using a broadband femtosecond optical parametric oscillator," Appl. Phys. Lett. **85**, 3366-3368 (2004).

[18]   C. Erny, K. Moutzouris, J. Biegert, D. Kühlke, F. Adler, A. Leitenstorfer, and U. Keller, "Mid-infrared difference-frequency generation of ultrashort pulses tunable between 3.2 and 4.8 μm from a compact fiber source," Opt. Lett. **32**, 1138-1140 (2007).

[19]   I. Galli, S. Bartalini, P. Cancio, F. Cappelli, G. Giusfredi, D. Mazzotti, N. Akikusa, M. Yamanishi, and P. De Natale, "Mid-infrared frequency comb for broadband high precision and sensitivity molecular spectroscopy," Opt. Lett. **39**, 5050-5053 (2014).

[20]   A. Gambetta, R. Ramponi, and M. Marangoni, "Mid-infrared optical combs from a compact amplified Er-doped fiber oscillator," Opt. Lett. **33**, 2671-2673 (2008).

[21] N. Leindecker, A. Marandi, R. L. Byer, and K. L. Vodopyanov, "Broadband degenerate OPO for mid-infrared frequency comb generation," Opt. Express **19**, 6296-6302 (2011)

[22] C. R. Phillips, J. Jiang, C. Mohr, A. C. Lin, C. Langrock, M. Snure, D. Bliss, M. Zhu, I. Hartl, J. S. Harris, M. E. Fermann, and M. M. Fejer, "Widely tunable mid-infrared difference frequency generation in orientation-patterned GaAs pumped with a femtosecond Tm-fiber system," Opt. Lett. **37**, 2928-2930 (2012).

[23] I. Hartl, "Thulium-fiber laser driven mid-infrared frequency combs," in *Advanced Solid-State Lasers Congress*, G. Huber and P. Moulton, eds., OSA Technical Digest (online) (Optical Society of America, 2013), paper AF1A.1.

[24] J. Faist, F. Capasso, D. L. Sivco, C. Sirtori, A. L Hutchinson, and A. Y Cho, "Quantum cascade lasers," Science **264**, 553-556 (1994).

[25] P. Q. Liu, A. J. Hoffman, M. D. Escarra, K. J. Franz, J. B. Khurgin, Y. Dikmelik, X. Wang, J.-Y. Fan and C. F. Gmachl, "Highly power-efficient quantum cascade lasers," Nature Photon. **4**, 95-98 (2010).

[26] Y. Yao, A. J. Hoffman, and C. F. Gmachl, "Mid-infrared quantum cascade lasers," Nature Photon. **6**, 432-439 (2012).

[27] B. Schwarz, P. Reininger, H. Detz, T. Zederbauer, A. M. Andrews, W. Schrenk, and G. Strasser, "Monolithically integrated mid-infrared quantum cascade laser and detector," Sensors **13**, 2196-2205 (2013).

[28] A. Hugi, G. Villares, S. Blaser, H. C. Liu, and J. Faist, "Mid-infrared frequency comb based on a quantum cascade laser," Nature **492**, 229–233 (2012).

[29] G. Villares, A. Hugi, S. Blaser, and J Faist, "Dual-comb spectroscopy based on quantum-cascade-laser frequency combs," Nat. Commun. **5**, 5192 (2014).

[30] C.Y. Wang, L. Kuznetsova, V. M. Gkortsas, L. Diehl, F. X. Kärtner, M. A. Belkin, A. Belyanin, X. Li, D. Ham, H. Schneider, P. Grant, C. Y. Song, S. Haffouz, Z. R. Wasilewski, H.C. Liu, and F. Capasso, "Mode-locked pulses from mid-infrared Quantum Cascade Lasers," Opt. Express **17**, 12929-12943 (2009).

[31] Y. Wang and A. Belyanin, "Active mode-locking of mid-infrared quantum cascade lasers with short gain recovery time," Opt. Express **23**, 4173-4185 (2015).

[32] Q. Y. Lu, M. Razeghi, S. Slivken, N. Bandyopadhyay, Y. Bai1, W. J. Zhou, M. Chen, D. Heydari, A. Haddadi, R. McClintock, M. Amanti, and C. Sirtori, "High power frequency comb based on mid-infrared quantum cascade laser at $\Box \sim 9 \Box$m," Appl. Phys. Lett. **106**, 051105 (2015).

[33] D. K. Armani, T. J. Kippenberg, S. M. Spillane, and K. J. Vahala, "Ultra-high-Q toroid microcavity on a chip," Nature **421**, 925-928 (2002).

[34] P. Del'Haye, A. Schliesser, O. Arcizet, T. Wilken, R. Holzwarth, and T. J. Kippenberg, "Optical frequency comb generation from a monolithic microresonator," Nature **450**, 1214–1217 (2007).

[35] A. A. Savchenkov, A. B. Matsko, V. S. Ilchenko, I. Solomatine, D. Seidel, and L. Maleki, "Tunable optical frequency comb with a crystalline whispering gallery mode resonator," Phys. Rev. Lett. **101**, 093902 (2008).

[36] A. A. Savchenkov, A. B. Matsko, W. Liang, V. S. Ilchenko, D. Seidel, and L. Maleki, "Kerr combs with selectable central frequency," Nature Photon. **5**, 293-296 (2011).

[37] P. Del Haye, T. Herr, E. Gavartin, M. L. Gorodetsky, R. Holzwarth, and T. J. Kippenberg, "Octave spanning tunable frequency comb from a microresonator," Phys. Rev. Lett. **107**, 063901 (2011).

[38] T. J. Kippenberg, R. Holzwarth, and S. A. Diddams, "Microresonator-based optical frequency combs," Science **332**, 555–559 (2011).

[39] A. B. Matsko, A. A. Savchenkov, D. Strekalov, V. S. Ilchenko, and L. Maleki, "Optical hyperparametric oscillations in a whispering-gallery-mode resonator: Threshold and phase diffusion," Phys. Rev. A **71**, 033804 (2005).

[40] T. Herr, K. Hartinger, J. Riemensberger, C. Y. Wang, E. Gavartin, R. Holzwarth, M. L. Gorodetsky, and T. J. Kippenberg, "Universal formation dynamics and noise of Kerr frequency combs in microresonators," Nature Photon. **6**, 480-487 (2012).

[41] A. A. Savchenkov, A. B. Matsko, W. Liang, V. S. Ilchenko, D. Seidel, and L. Maleki, "Kerr frequency comb generation in overmoded resonators," Opt. Express **20**, 27290-27298 (2012).

[42] T. J. Kippenberg, S. M. Spillane, and K. J. Vahala, "Kerr-nonlinearity optical parametric oscillation in an ultrahigh-Q toroid microcavity," Phys.Rev. Lett. **93**, 083904 (2004).

[43] C. Wang, T. Herr, P. Del Haye, A. Schliesser, J. Hofer, R. Holzwarth, T. Hänsch, N. Picque, and T. Kippenberg, "Mid-infrared optical frequency combs at 2.5 □m based on crystalline microresonators, Nat. Commun. **4**, 1345 (2013).

[44] A. G. Griffith, R. K.W. Lau, J. Cardenas,Y. Okawachi, A. Mohanty, R. Fain, Y. H. D. Lee, M. Yu, C. T. Phare, C. B. Poitras, A. L. Gaeta , and M. Lipson, "Silicon-chip mid-infrared frequency comb generation," Nat. Commun. **6**, 6299 (2015).

[45] I. H. Agha, Y. Okawachi, and A. L. Gaeta, "Theoretical and experimental investigation of broadband cascaded four-wave mixing in high-Q microspheres," Opt. Express **17**, 16209 (2009).

[46] W. Liang, A. A. Savchenkov, A. B. Matsko, V. S. Ilchenko, D. Seidel, and L. Maleki, "Generation of near-infrared frequency combs from a MgF_2 whispering gallery mode resonator," Opt. Lett. **36**, 2290-2292 (2011).

[47] M. L. Gorodetsky and V. S. Ilchenko, "Optical microsphere resonators: optimal coupling to high-*Q* whispering-gallery modes," J. Opt. Soc. Am. B **16**, 147-154 (1999).

[48] T. Carmon, L. Yang, and K. J. Vahala, "Dynamical thermal behavior and thermal self-stability of microcavities," Opt. Express **12**, 4742-4750 (2004).

[49] W. Liang, V. S. Ilchenko, A. A. Savchenkov, A. B. Matsko, D. Seidel, and L. Maleki, "Whispering-gallery-mode-resonator-based ultra-narrow linewidth external-cavity semiconductor laser," Opt. Lett. **35**, 2822-2824 (2010).

[50] S. B. Papp and S. A. Diddams, "Spectral and temporal characterization of a fused-quartz-microresonator optical frequency comb," Phys. Rev. A **84**, 053833 (2011).

[51] L. Maleki, V. S. Ilchenko, A. A. Savchenkov, and A. B. Matsko, "Crystalline Whispering Gallery Mode Resonators in Optics and Photonics", Chapter 3 in *Practical Applications of Microresonators in Optics and Photonics* edited by A. B. Matsko, (CRC Press, 2009).

[52] A. Coillet, I. V. Balakireva, R. Henriet, K. Saleh, L. Larger, J. M. Dudley, C. R. Menyuk, Y. K. Chembo, "Azimuthal Turing Patterns, Bright and Dark Cavity Solitons in Kerr Combs Generated With Whispering-Gallery-Mode Resonators," IEEE Photon. J. **5**, 6100409 (2013).

[53] C. Godey, I. V. Balakireva, A. Coillet, and Y. K. Chembo, "Stability analysis of the spatio-temporal Lugiato-Lefever model for Kerr optical frequency combs in the anomalous and normal dispersion regimes," Phys. Rev. A **89**, 063814 (2014).

[54] F. Ferdous, H. X. Miao, D. E. Leaird, K. Srinivasan, J. Wang, L. Chen, L. T. Varghese, and A. M. Weiner, "Spectral line-by-line pulse shaping of on-chip microresonator frequency combs," Nature Photon. **5**, 770776 (2011).

[55] K. Mansour, A. S. Rury, I. S. Grudinin, and N. Yu, "Progress towards whispering gallery mode resonator based spectroscopy in mid-infrared," Proc. SPIE **8960**, 89600Y (2014).

[56] M. L. Gorodetsky and V. S. Ilchenko, "High-Q optical whispering gallery microresonators: precession approach for spherical mode analysis and emission patterns with prism couplers," Opt. Comm. 113, 133-143 (1994).

5. Personnel Supported

    a.   Dr. Wei Liang

    b.   Dr. Anatoliy Savchenkov

    c.   Dr. Andrey Matsko

d. Dr. Fabio Di Teodoro

6. Publications

1. Mario Siciliani de Cumis, Simone Borri, Giacomo Insero, Iacopo Galli, Anatoliy Savchenkov, Danny Eliyahu, Vladimir Ilchenko, Naota Akikusa, Andrey Matsko, Lute Maleki, and Paolo De Natale, "Microcavity-Stabilized Quantum Cascade Laser," in preparation.

2. W. Liang, D. Eliyahu, V. S. Ilchenko, A. A. Savchenkov, A. B. Matsko, D. Seidel & L. Maleki, "High spectral purity Kerr frequency comb radio frequency photonic oscillator," Nature Communications 6, Article number: 7957 (2015) doi:10.1038/ncomms8957

3. Anatoliy A. Savchenkov, Vladimir. S. Ilchenko, Fabio Di Teodoro, Paul M. Belden, William T. Lotshaw, Andrey B. Matsko, and Lute Maleki, "Generation of Kerr combs at 4.5um in crystalline microresonators pumped by quantum-cascade lasers," Opt. Lett. 40, 3468-3471 (2015); doi: 10.1364/OL.40.003468

4. W. Liang, A. A. Savchenkov, Z. Xie, J. F. McMillan, J. Burkhart, V. S. Ilchenko, C. W. Wong, A. B. Matsko, and L. Maleki, "Miniature multioctave light source based on a monolithic microcavity," Optica 2, 40-47 (2015). doi: 10.1364/OPTICA.2.000040

5. Andrey B. Matsko and L. Maleki, "Noise conversion in Kerr comb RF photonic oscillators," J. Opt. Soc. Am. B 32, 232-240 (2015). doi: 10.1364/JOSAB.32.000232

6. B. Bao, L. Zhang, A. Matsko, Y. Yan, Z. Zhao, G. Xie, A. M. Agarwal, L. C. Kimerling, J. Michel, L. Maleki, and A. E. Willner, "Nonlinear conversion efficiency in Kerr frequency comb generation," Opt. Lett. 39, 6126-6129 (2014); http://dx.doi.org/10.1364/OL.39.006126

7. F. Ferdous, A. A. Demchenko, S. P. Vyatchanin, A. B. Matsko, and L. Maleki "Microcavity morphology optimization," Phys. Rev. A 90, 033826 (2014); DOI: http://dx.doi.org/10.1103/PhysRevA.90.033826

8. V. S. Ilchenko, A. A. Savchenkov, A. B. Matsko, and L. Maleki, "Generation of Kerr frequency combs in a sapphire whispering gallery mode microresonator," Opt. Eng. 53(12), 122607 (Aug 20, 2014), http://dx.doi.org/10.1117/1.OE.53.12.122607

9. W. Liang, A. A. Savchenkov, V. S. Ilchenko, D. Eliyahu, D. Seidel, A. B. Matsko and L. Maleki "Generation of a coherent near-infrared Kerr frequency comb in a monolithic microresonator with normal GVD," Optics Letters 39 (10), 2920-2923 (2014). http://dx.doi.org/10.1364/OL.39.002920

10. Andrey B. Matsko and L. Maleki, "On timing jitter of mode locked Kerr frequency combs," Optics Express 21 (23), 28862-28876 (2013). http://dx.doi.org/10.1364/OE.21.028862

Contract No:
FA9550-12-C-0068   OEwaves, Inc.   38

Distribution Statement A. Approved for public release, distribution is unlimited.

11. V. S. Ilchenko, A. M. Bennett, P. Santini, A. A. Savchenkov, A. B. Matsko, L. Maleki, "Whispering gallery mode diamond resonator," Optics letters 38 (21), 4320-4323 (2013). http://dx.doi.org/10.1364/OL.38.004320

12. Andrey B. Matsko, W. Liang, A. A. Savchenkov, and L .Maleki, "Chaotic dynamics of frequency combs generated with continuously pumped nonlinear microresonators," Optics Letters 38 (4), 525-527 (2013). http://dx.doi.org/10.1364/OL.38.000525

13. Anatoliy A. Savchenkov, A. B. Matsko, W. Liang, V. S. Ilchenko, D. Seidel, and L. Maleki, "Kerr frequency comb generation in overmoded resonators," Opt. Express 20, 27290-27298 (2012); http://dx.doi.org/10.1364/OE.20.027290

14. Andrey B. Matsko, A. A. Savchenkov, and L. Maleki, "On excitation of breather solitons in an optical microresonator," Opt. Lett. 37, 4856-4858 (2012); http://dx.doi.org/10.1364/OL.37.004856

15. Anatoliy Savchenkov, A. B. Matsko, W. Liang, V. S. Ilchenko, D. Seidel, and L. Maleki, "Transient regime of Kerr-frequency-comb formation," Phys. Rev. A 86, 013838 (2012); http://dx.doi.org/10.1103/PhysRevA.86.013838

7. Interactions/Transitions

Participation/presentations at meetings, conferences, seminars, etc.

1. A. B. Matsko, a presentation at AFOSR- Ultra-Short Pulse Laser-Matter Interactions Program Review Meeting, December 18-20, 2012

2. A. B. Matsko, A. A. Savchenkov, and L. Maleki, "Hyper-Parametric Oscillations in Multimode Microresonators," 2012 IEEE Photonics Conference, 23 - 27 September 2012.

3. A. B. Matsko, Lecturing at 7th Optoelectronics & Photonics Winter School: "Physics and Applications of Optical Resonators," 16th - 22nd of March, 2013, Levico Terme (Trento, Italy).

4. V. Ilchenko, J. Byrd, A. Savchenkov, D. Eliyahu, W. Liang, A. B. Matsko, D. Seidel, and L. Maleki, "Kerr Frequency Comb-Based Ka-band RF Photonic Oscillator," 2013 IEEE—UFFC joint symposia on 21—25 July 2013, Prague, Czech Republic, paper IFCS-EFTF2-A2-2 (2013).

5. A. B. Matsko, and L. Maleki, " Partially Coherent Kerr Frequency Combs," OSA Nonlinear Optics, Kohala Coast, Hawaii, July 21-26, 2013.

6. W. Liang, A. Savchenkov, J. McMillan, Z. Xie, V. Ilchenko, D. Seidel, C. W. Wong, A. B. Matsko, and L. Maleki, "Strongly Nondegenerate Resonant Optical Parametric Oscillator," OSA Nonlinear Optics, Kohala Coast, Hawaii, July 21-26, 2013.

7. Y. Yan, A. Matsko, C. Bao, L. Maleki, and A. E Willner, "Increasing the Spectral Bandwidth of Optical Frequency Comb Generation in a Microring Resonator using Dispersion Tailoring Slotted Waveguide," 2013 IEEE Photonics Conference (IPC), 230-231 (2013).

8. Vladimir S. Ilchenko, Anatoliy A. Savchenkov, Andrey B. Matsko, Lute Maleki, "Crystalline whispering gallery mode resonators: in search of the optimal material," Photonics West 2014, Paper 8960-38 (2014); Proc. SPIE vol. 8960, pp. 896013-896013-10 (2014).

9. Wei Liang, Danny Eliyahu, Andrey B. Matsko, Vladimir S. Ilchenko, David J. Seidel, Lute Maleki, "Spectrally pure RF photonic source based on a resonant optical hyper-parametric oscillator," Photonics West 2014, Paper 8960-35 (2014); Proc. SPIE vol. 8960, pp. 896010-896010-8 (2014).

10. A. B. Matsko, a presentation at AFOSR- Ultra-Short Pulse Laser-Matter Interactions Program Review Meeting, May 29, 2014

Transitions

The knowledge resulting from the effort is used in the development of a packaged RF photonic oscillator, development of which is supported by Phase II of DARPA SBIR "Integrated Ultra-high Performance Oscillator Based on a Crystalline Kerr Comb" Contract # W911QX-12-C-0067 (OEwaves and UC Davis, PI: A. B. Matsko)

8. New discoveries, inventions, or patent disclosures
None

9. Honors/Awards
a. A. B. Matsko became an OSA Fellow and APS Outstanding Referee in 2013.